NTNU
Det skapende universitet

Alumina supported cobalt catalysts for Fischer-Topsch synthesis

Amir Shadman Far

Industriell kjemi og bioteknologi
Innlevert: August 2012
Hovedveileder: Anders Holmen, IKP
Medveileder: Andreas Helland Lillebø, IKP

Norges teknisk-naturvitenskapelige universitet
Institutt for kjemisk prosessteknologi

NTNU
Norwegian University of Science and Technology

Faculty of Natural Sciences and Technology
Department of Chemical Engineering

MASTER THESIS 2012

Title: : Alumina Supported Cobalt Catalysts for Fischer-Tropsch Synthesis	**Subject (3-4 words): Catalyst Characterization, F-T Synthesis**
Author: Amir Shadman Far	**Carried out through: NTNU**
Advisor: Anders Holmen **Co-advisor: Andreas Hellan Lillebø** **External advisor:**	**Number of pages** **Main report: 44** **Appendix: 3**

ABSTRACT: Fischer-Tropsch Synthesis Alumina phasesAlpha, Theta, Delta and Gamma Al_2O_3 were produced from a small and a medium pore Alpha Al_2O_3 by heat treatment. All catalysts were prepared by incipient wetness impregnation resulting in a cobalt, Rhenium and Platinum loading of 12, 0.5 and 0.5wt.% respectively. Two of the catalysts were tested in a fixed bed reactor at 20 bar, 483 K and H_2/CO = 2.1.

Goal of work (key words): Fischer-Tropsch Synthesis; Cobalt; Rhenium; Platinum; Alumina; C5+ Selectivity; Catalyst activity.

Conclusions and recommendations (key words): Metal promoter precursors containing chlorine Results in law metal dispersion due to surface coverage by Chlorine. The catalyst Activity increasing due to chlorine removal from the surface during the F-T Reaction. It is not recommended to use promoter precursors containing Chlorine.

I declare that this is an independent work according to the exam regulations of theNorwegian University of Science and Technology

Date and signature: 31.08.2012 Amir Shadman Far

Acknowledgements

I would like to mention those people who helped me in this project and gave me advices. First of all I would like to thank my supervisor professor Anders Holmen for his help and my co-supervisor Andreas Helland Lillebø for his continuous help. Many thanks to Julian Tolchard from institue of material technology for his advices and help in characterization of the samples.

Finally I would like to thank my family for encouraging me and be there when I needed them. Thanks to those master students whom I worked with and those whom I forgot to mention here

. **Abstract**

In Fischer-Tropsch synthesis (FT) there are many metal catalysts that have been in use and tested. Among these cobalt catalysts are preferred due to their high yields of straight-chain alkanes. Cobalt metal is loaded on a support by impregnation method. Support should have proper properties and it plays an important role in FT synthesis. Alumina (Al_2O_3) is one of the candidates for this purpose. Alumina (Al_2O_3) phases were used for investigation of Fischer-Tropsch synthesis. Different alumina phases can be prepared from (gamma) alumina phase by heat treatment of gamma phase which is the initial phase. All alumina phases were medium pore aluminas denoted (MP) alumina. The reason back choosing medium pore alumina was the high C_{5+} selectivity for the medium pore alumina. The alumina phases prepared from the initial phase were alpha and theta phases.

The alumina supported rhenium promoted cobalt catalysts were prepared by one-step incipient wetness impregnation to give 12 wt% cobalt and 0.5 wt% rhenium. Since the Co_3O_4 particle sizes were held constant, no ethylene glycol was used during the impregnation step. For the catalysts cobalt nitrate hexahydrate and perrhenic acid were used as cobalt and rhenium precursor, respectively. The impregnation was followed by drying, calcination and in situ reduction. The catalyst sample was sieved in order to obtain particles in size range of 53-90 μm.

The prepared catalyst samples then were characterized by standard H_2-chemisorption and temperature-programmed reduction.

During the calcination step, the calcination atmosphere and temperature were remained constants for both catalyst samples. The goal of the calcination step is to decompose the cobalt nitrate hydrate and obtain cobalt oxide particles (Co_3O_4). During the reduction step the Co_3O_4 particles were expected to be reduced completely yield cobalt metal in two steps via an intermediate CoO.

Nomenclature

Symbol	Discription
α	Alpha alumina
γ	Gamma alumina
θ	Theta alumina
δ	Delta alumina
κ	Kappa alumina
MP	Medium pore
TPR	Temperature programmed reduction
XRD	X-ray diffraction
FT	Fischer-Tropsch
t	Co_3O_4 crystallite thickness in nm
K	shape factor (0.89)
B	Full with half maximum of Co_3O_4 peak at $2\Theta=36.9°$
b	Instrumental width of the LaB_6 at $2\Theta=35.5°$
λ	Wave length
$\mathbf{V_{ads}}$	volume of hydrogen adsorbed in cm^3/g STP
D%	Co metal dispersion
$\mathbf{wt_{Co}}$	wt.% of cobalt
$\mathbf{W_{Co°}}$	Atomic weight of cobalt
$\mathbf{A_{Co}}$	Area of cross section of cobalt atom $=0.66\ nm^2$
$\mathbf{N_A}$	Avogadro's number $= 6.023.10^{23}$
ρ	Density of cobalt $= 8.9\ g/cm^3$
S/V	Surface to volume eation
SCo°	Metallic surface area, m^2/g
ε	Porosity
$\mathbf{r_p}$	Pore radius
TOF	Turn over Frequency

Contents

List of figures

List of tables

"If the world's ethical standards fail to raise with the advances of our technological revolution, the world will go to hell. Let us remember that in the horse-and-buggy days nobody got hurt if the coachman had a drink too many. In our times of high-powered automobiles, however, that same drink may be fatal....“

Werner von Braun (constructed the V-2 rocket, but also the Saturn V)

Chapter 1

1. Introduction

Today in this century there is a strong demand on energy due to fast growth in both population and industrial development. Figure(1).

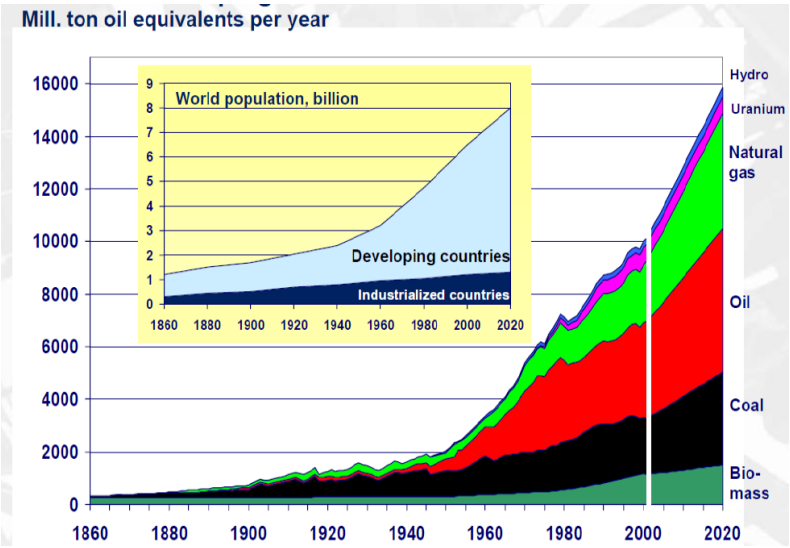

Figure 1 world energy consumption and population increase [1]

The major source of energy still is fossil energy represented by oil, gas, coal and biomass. In recent years natural gas has gained higher attention since natural gas is more evenly distributed than oil. Natural gas is more environmental friendly than crude oil and can be a better source of energy. Crude oil contains higher amount of impurities such as sulphur compounds, heavy metals (Ni, V) which is lower in natural gas and easier to handle. The technology for converting gas to liquid fuel has had a tremendous development and this made the Gas to Liquid conversion an important solution.

1.1 Gas - to- Liquid

The main dependency in production of fuel and chemicals still is on crude oil as an energy source. The major sector with highest energy demand is transportation sector. Figure(1.1.1).

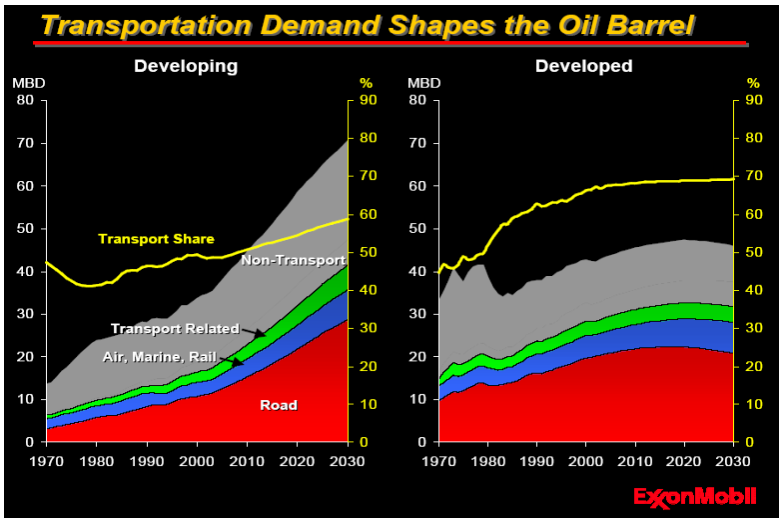

Figure1.1.1 Transportation demand [2]

Transport expected to account for 60-70% of crude oil demand. Since the oil production has already passed its peak, the production now is on its way to decline see figure (1.1.2). As it is clear from the figure (1.1.2), the production of crude oil is on its way to decline, this requires other sources of energy. Natural gas resources have the capacity to produce natural gas for longer time than crude oil resources; this explains that natural gas could be a reliable source of energy in for longer time in the future. Figure (1.1.3) and (1.1.5). In order to cover the increasing demand on energy; other energy sources are of interest. In contrast to crude oil which contains a wide range of hydrocarbons, natural gas consists mainly of methane and small amounts of ethane, propane, butane etc. see Figure (1.1.4).

Natural gas, coal and biomass are other sources for production of liquid fuel using GTL, CTL and BTL technology respectively.

The transportation of natural gas to markets either by pipeline or in liquid form as liquefied natural gas (NGL) by ships or tankers is difficult and expensive. It is therefore beneficial to convert the gas to liquid fuels or liquid chemicals such as diesel, ammonia or methanol, which are easier to transport.

Fischer-Tropsch synthesis products are diesel and naphtha, and these products have unlimited market. The interest in GTL technology is not only because of abundant resources and supply of natural gas. But also the products are cleaner and more pure, and are environmentally more beneficial than transportation fuels derived from crude oil which contain more impurities such as nitrogen, aromatics and metals.

Table (1.1.1) shows a comparison between FT synthesized diesel and other types of diesel.

Table 1.1.1 FT diesel properties vs EU & US specifications [4]

Properties	GTL diesel	EU(2005)	US(2006)
Maximum sulphur(ppm)	0	50/10	15
Boiling point range(C°)	150-360	180-360	180-360
Minimum cetane number	70	51	40
Maximum aromatic (vol%)	0	N.A	35
Maximum density (kg/l)	0.79	0.845	0.876

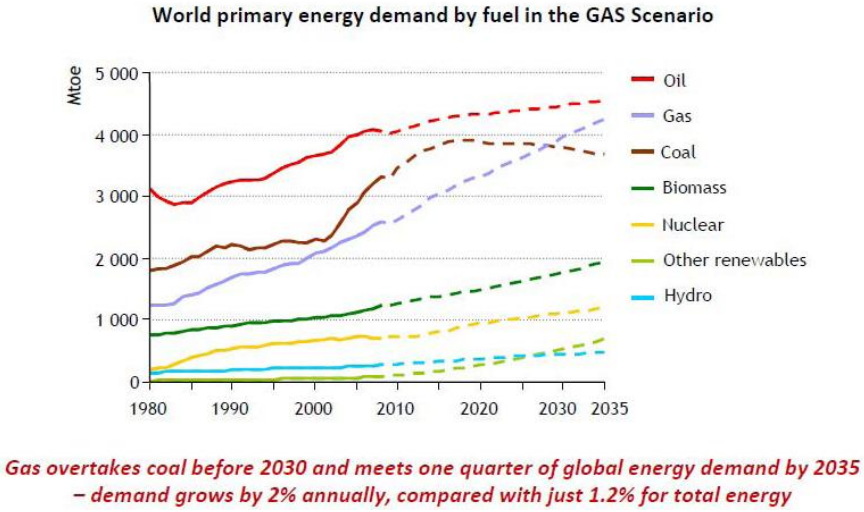

Figure 1.1.5 world primary energy demands [1]

1.2 History

The first pioneers in converting CO to liquid products were Losanitsch and Jovitschitsch [7] who converted CO and hydrogen using an electric discharge with no catalyst involved in 1897. Sabatier and Senderens produced methane from CO and hydrogen over nickel catalyst early in 1920. Many years after them Franz Fischer and Hans Tropsch developed chemistry and process for production of hydrocarbon liquids and paraffins over iron Fe and cobalt Co catalyst at atmospheric pressure at 250-300 C°

Until recently, it was not possible for GTL based fuels to compete with conventional crude oil based fuels. In fact that crude oil price was low and GTL technology was not of interest until the oil price started to incline . Special cases were during World War II when Germany

needed liquid fuels and used FT synthesis to produce liquid fuels from coal derived syn gas [8]. And the apartide regime in South Africa to reduce dependency on imported oil (Sasol). There are not many large scaled gases to liquid plants in these days, only a few plants produce more than 1000bbl/day. The petro SA plant in South Africa and shell GTL plant in Malaysia are largest examples. Sasol is building a large scale plant in Qatar with a production rate 34,000 bbl/d of liquid fuels [6].

Table 1.2.1 shows current GTL plants.

Table 1.2.1 Status of existing plant [6]

Location	Company	Production(BPD)	Status
Mossel Bay, South Africa	Petro SA	30,000	Operating
Bintulu, Malaysia	Shell	14,500	Operating
Oryx GTL, Qatar	Sasol	34,000	Operating
Pearl GTL, Qatar	Shell	140,000	Start-up phase
Escravos, Nigeria	Chevron	34,000	Under construction

1.3 Fischer – Tropsch Technology

There are three main steps involved in the GTL process. These are:

- Synthesis gas production
- Fischer- Tropsch synthesis
- Product upgrade

Fischer-Tropsch synthesis and product upgrade as shown in figure 1.3.1.

In the first step the synthesis gas is produced, here the synthesis gas (syn gas) is derived from natural gas. The technologies to produce syn gas are steam reforming, partial oxidation and autothermal reforming. In the autothermal reforming both reforming and partial oxidation of natural gas are combined. Part of the feed (natural gas) is burned to provide heat for the endothermic reforming reaction. This combination is attractive and economical today. The second step is the Fischer-Tropsch synthesis. This step is a catalytic reaction in which the sun gas is converted to liquid hydrocarbon (paraffin and olefins with different chain length) over a catalyst. The product distribution is shown in table 1.3.1.

In upgrading step some reactions are involved in order to improve the quality and properties if the products according to specifications. Such reactions are hydrocracking and hydro isomerisation. The final products will be separated into naphtha, diesel, kerosene, jet fuel and residue.

Figure 1.3.1 Main steps in GTL process

Table 1.3.1 GTL products [6]

Name	Compound
Fuel gas	C1-C2
Liquefied petroleum gas	C3-C4
Gasoline	C5-C12
Naphtha	C8-C12
Kerosene(jet fuel)	C11-C13
Diesel	C13-C17
Middle distillates	C10-C20
Soft wax	C19-C23
Medium wax	C24-C35
Hard wax	C35+

A simple Fischer-Tropsch synthesis process flow diagram is presented in figure (1.3.2).

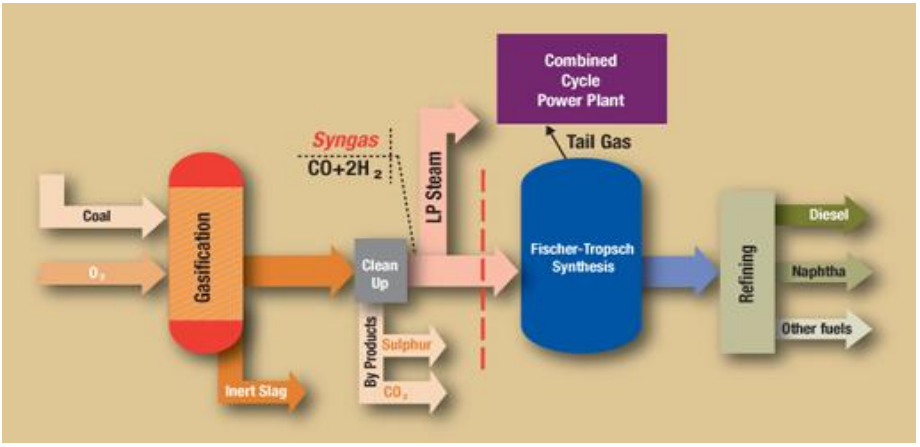

Figure 1.3.2 a simple F-T synthesis process flow diagram [9]

1.3.1 Fischer –Tropsch synthesis

In the FT synthesis CO reacts with hydrogen to produce a mixture of higher hydrocarbons. The industrial conditions vary with the type of the catalyst chosen.
There are both low temperature (LTFT) and high temperature (HTFT) Fischer-Tropsch synthesis. The operation temperature of the latest one (HTFT) is from 330C˚- 350C˚ and the catalyst used is iron based catalyst. This process is used in Coal To Liquid technology (CTL).The first one (LTFT) operates at lower temperature and uses cobalt based catalyst and used in Gas To Liquid process (GTL).

1.3.2 Reactions

The FT reactions are very exothermic and the heat released is ΔH ≈ -165 kJ/mole CO converted. Typical FT conditions are 190C˚ - 300 C˚.
The fundamental main reactions in the FT synthesis are presented below:
Main and side reactions in F-T synthesis [6].

Main reactions	
Alkanes	$n\mathrm{CO} + (2n + 1)\mathrm{H_2} \rightarrow \mathrm{C}_n\mathrm{H}_{2n+2} + n\mathrm{I_2O}$
Alkenes	$n\mathrm{CO} + 2n\mathrm{H_2} \rightarrow \mathrm{C_2H}_{2n} + n\mathrm{H_2O}$
Water-gas shift	$\mathrm{CO} + \mathrm{H_2O} \rightleftarrows \mathrm{CO_2} + \mathrm{H_2}$
Side reactions	
Alcohols	$n\mathrm{CO} + 2n\mathrm{H_2} \rightarrow \mathrm{H(-CH_2-)}_n\mathrm{OH} + (n-1)\mathrm{H_2O}$
Boudouard reaction	$2\mathrm{CO} \rightarrow \mathrm{C} + \mathrm{CO_2}$

The formation of the products occurs in a polymerisation reaction, and there are different mechanisms proposed. The most accepted one is the carbon mechanism which involves the insertion of $–CH_2-$ in to a growing chain. The mechanism is shown in figure 1.3.2.1 bellow.

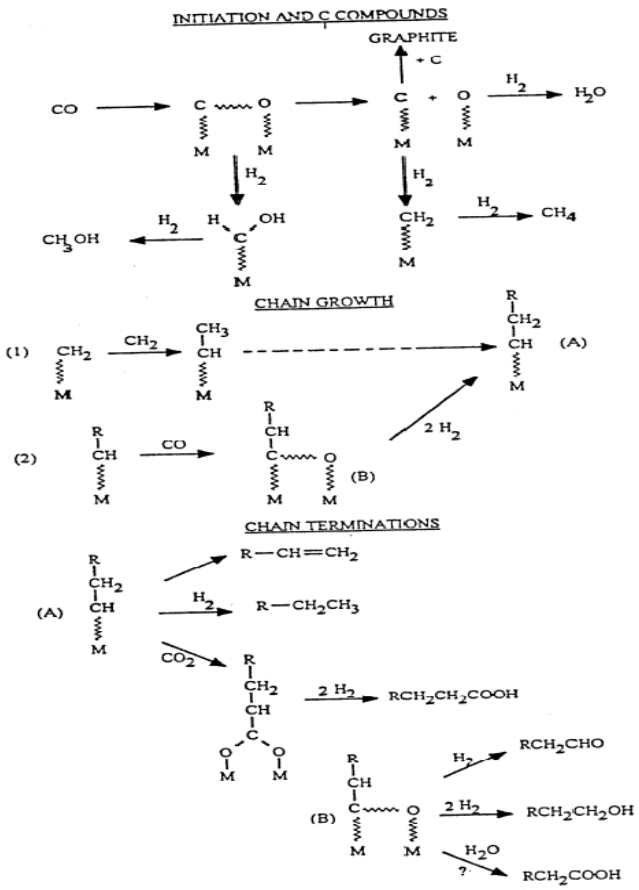

Figure 1.3.2.1 Mechanism of FT reaction [6]

1.3.3 Catalyst candidates

Group VIII metals show an interesting activity, especially iron, nickel, cobalt and ruthenium. The choice of catalyst for FT synthesis is linked to some factors such as the price of the active metal, the products, and the feed source. From the metals mentioned above, ruthenium is the most expensive and less available [10]. This makes the ruthenium less favourite candidate for FT synthesis.

Nickel is suitable for methane production, and when used in FT synthesis nickel forms volatile carbonyls. Thus nickel is not the most favourite catalyst for Ft synthesis.

Iron based catalysts show high water-gas-shift activity, thus suitable for synthesis gas with low H_2/CO ration, as in case of coal as the source for carbon.

Cobalt has a low water-gas-activity and hence mush used in FT synthesis when natural gas is used to derive syngas.

Supports like AL_2O_3, SiO_2 and TiO_2 are used to be loaded with cobalt and increase the exposure of cobalt.

1.3.4 Reactors

As mentioned previously the FT reactions are exothermic and large amount of heat is released. It is therefore a major consideration to remove heat in an efficient way in the design of the reactors. This is achieved through heat exchanging with water. The most currently used reactors are: Figure 1.3.4.1

- Multi tubular fixed bed reactor
- Riser reactor
- Slurry reactor

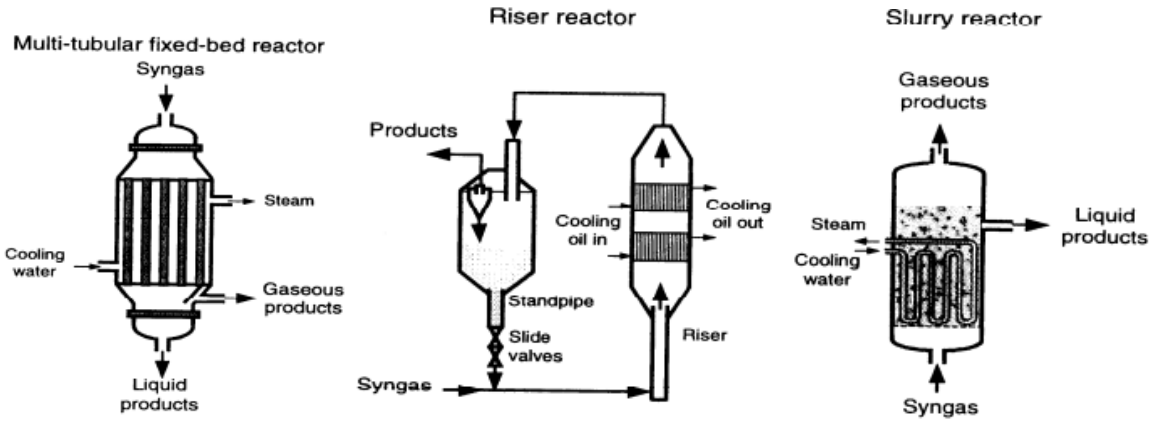

Figre 1.3.4.1 Reactors used for Fischer-Tropsch synthesis [6]

Chapter 2

Literature review

There are three metals i.e. Ru, Co, Fe that can be used in Fischer-Tropsch synthesis and possess high activity to produce long chain hydrocarbons. The precursors of these elements are in acetate, nitrate or chlorides form and are deposited on different supports. Inorganic materials or salts that have high surface area are used as supports, such as alumina, silica, titania, carbon nanofibers, ceria, zeolites, hydrotalcite, silicon carbide, niobia and natural clay.

Alumina is thermal stabil during reaction condition and therefore is interesting as support. Cobalt metal is viable the low in cost compared to above mentioned metals and deactivates slowly and also the interaction of cobalt with alumina and no water-gas-shift activity make alumina supported cobalt a good option as catalyst in Fischer-Tropsch synthesis.

Different types of alumina phases exist and can be obtained from minerals such as Gibbsite, Boehmite, Bayerite and Diaspore [11]. Different phases of alumina exist and they are γ-,η-, α-,δ-,θ-, κ- and λ- Al_2O_3.

The catalystic performance of the F-T catalyst can be enhanced by promotion with noble matals such as Ru, Pd, Pt and Re.

The noble metal promoters have a vriety effect on the structure of the F-T cobalt catalysts, cobalt metal dispersion and reducibility og the cobalt. The reducibility of the promoted cobalt oxides is carried out at lower temperature in Temperature-Programmed-Reduction compared to unpromoted cobalt catalysts.

2.1 Preparation of Fischer-Tropsch catalysts

Alumina support can be prepared in any desired phase by the heat treatment of the parent γ- Al_2O_3. A cobalt alumina supported catalyst can be prepared by the method of incipient wetness impregnation. The alumina support is impregnated with an aqueous solution of cobalt nitrate hexahydrate which is cobalt precursor. This step is followed by drying and calcination to make the cobalt nitrate hydrate

decompose and a cobalt oxide is obtained. During the calcination step, the condition such as heating rate has a significant effect on the performance of the catalyst.(Loosdrecht et al). According to van de Loosdrecht et al. lower heating rate decreases water and NO_x concentration at the catalyst during the calcination which positively affects the catalytic performance in Fischer-Tropsch synthesis. The in situ reduction of the cobalt oxide catalyst which is inactive is transformed to an active metallic cobalt. All steps are illustrated in figure (2.1).

The catalyst properties such as cobalt metal dispersion is influenced by several factors. These factors can be metal precursor, support mineral and calcination conditions in term of temperature and type of gas used [12]. Cobalt particle size and surface area of metallic cobalt can be affected by noble metal promoters (Ru, Pd, Pt, Re) in the reduced catalyst.

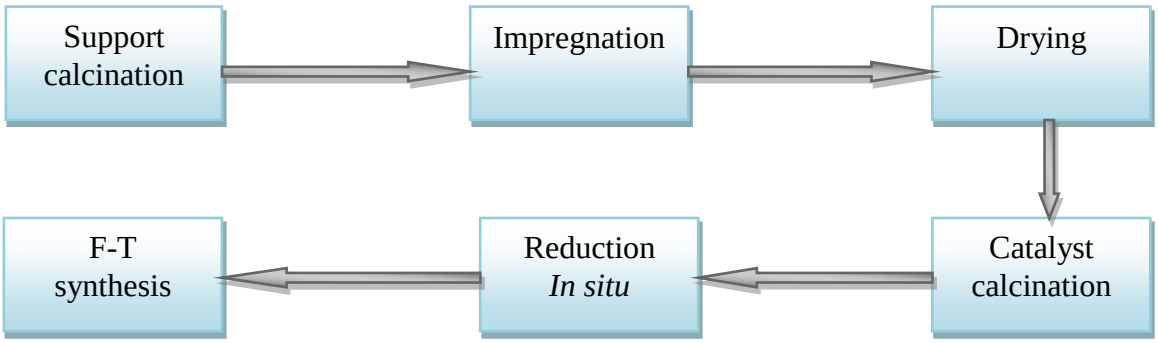

Figure 2.1 Catalyst preparation steps [14]

2.2 Temperature programmed reduction

Cobalt oxide is inactive and therefore must be reduced to active metallic cobalt by reduction. The reduction process takes place in two steps. The first step involves reduction of Co_3O_4 to CoO and second step reduction of CoO to Co as shown in the following reactions:

$$Co_3O_4 + H_2 \rightarrow 3CoO + H_2O \quad (2.2.1)$$

$$3CoO + 3H_2 \rightarrow 3Co° + 3H_2O \quad (2.2.2)$$

[14]. In reduction of alumina supported cobalt catalysts, incomplete reduction has been repported. This incomplete reduction is due to metal support interaction and formation of

cobalt complex compund and insertion of cobalt ions into the support.This metal support interaction increases in the order as γ- Al_2O_3 > TiO_2 > SiO_2. Modification of the support can change the reducibility [13]. Zhang et al treated γ- Al_2O_3 support in different media and found that reducibility is varied. The role of the metal promoters is facilitating the reduction of smaller CoO particles. The reduction depends also on Co_3O crystallite size and at the end reducibility of the catalyst is affected by support such as γ- Al_2O_3, TiO_2 and SiO_2.

The reducibility is also dependant of cobalt precursor, cobalt loading, and preparation method [14].

2.3 Mechanism of Fischer-Tropsch synthesis

The Fischer-Tropsch synthesis yields a wide range of hudrocarbon products. Products molecular weight distribution depends on the catalyst, the temperature and the pressure. The hydrocarbons are formed by a chain growth process,figure(2.3.1) and the length of the chain is determined by the selectivity of the catalyst and the conditions during the reaction.

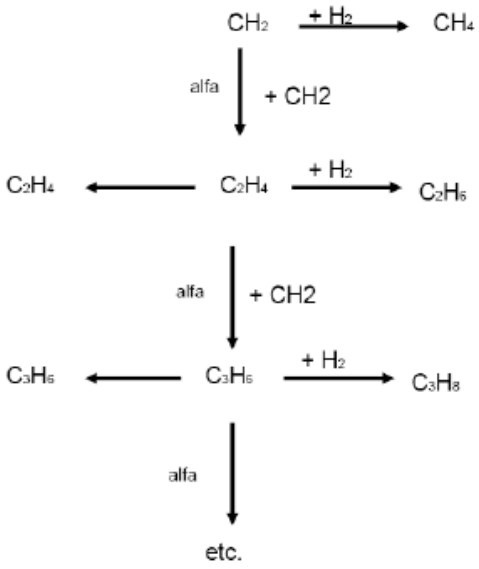

Figure 2.3.1 Chain growth mechanism for F-T synthesis [6]

In the Fischer-Tropsch synthesis the selective production of hydrocarbons rather than methane is difficult or not possible. A mixture of hydrocarbons with different chain length is formed and. See figure (2.3.2).

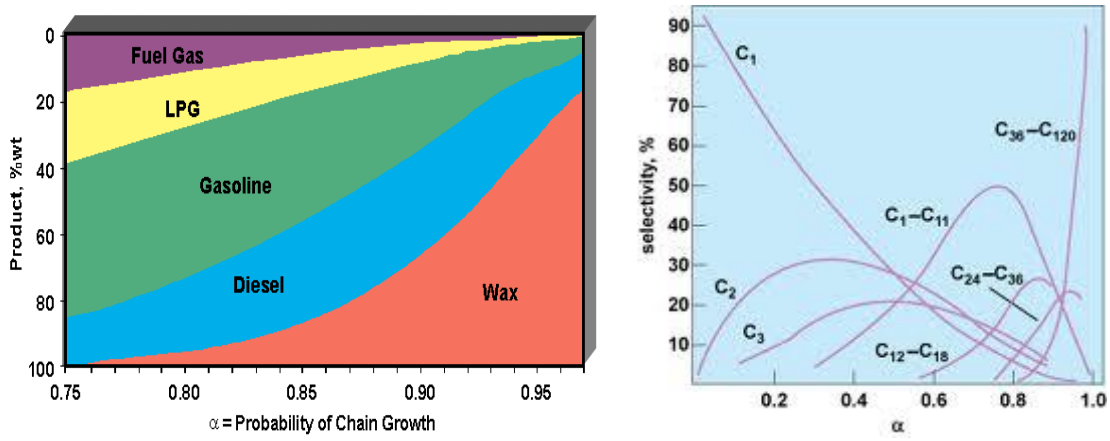

Figure 2.3.2 Hydrocarbon distribution based on chain growth probability [6]

An approporiate choice of catalyst and reaction conditions can shift the chain growth probability so different products can be formed [6]. The distribution of products according to carbon number can be represented by a statical model known as the Anderson-Flory-Schulz distribution. This model is presented as following:

$$\frac{W_n}{n} = (1-\alpha)^2 \alpha^{n-1}$$

Where W_n is the weight fraction of the product containing 'n' varbon atoms, and 'α 'is the chain growth probability and is defined as the ration of rate of propagation (r_p) to the rate of propagation (r_p) and rate of termination (r_t) of the growing chain:

$$\alpha = \frac{r_p}{r_p + r_t}$$

According to figure (2.3.1) diesel and wax can be produced when the chain growth probability is high about 0.85 and higher and methane at very low chain growthe the probability. Thus methane and wax are the only products that can be produced with 100% selectivity. The synthesis reaction can be considered as a polymerization mechanism involving several steps shown as following:

- Reactant adsorption which is the first step
- Chain initiation
- Chain growth
- Chain termination
- Product desorption

What is important to mention here is that mass transfer affects the F-T synthesis. In FT synthesis the reactants are in gas phase but however the pores in the catalyst will be filled

with liquid namely water and wax formed from the reaction. The diffusion in the liquid phase is slower than in the gas phase and this makes even slow reactions mass transfer limited something that influence the selectivity and activity.

The diffusion limitation reactions fall mainly into two types, namely diffusion limited CO arrival and diffusion limited removal of the reactive products.

The diffusion limited CO arrival is the reason for CO shortage at the catalytic sites and therfore the selectivity to long chain hydrocarbons is decreased since there is a CO shortage and no carbon to put in in the poplymerization reaction [12]. The diffusion limited removal of the reactive products leads to increased secondary reactions that can lead to increased α-olefin re-adsorption or α-olefin hydrogenation as shown in figure (2.3.3).

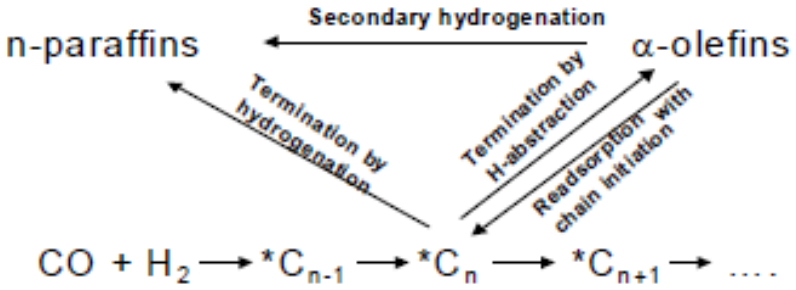

Figure 2.3.3 Reactions for F-T synthesis [12]

There are four different mechanisms proposed for F-T synthesis which are:

- Enol mechanism
- CO insertion
- Carbide mechanism
- Alkenyl mechanism

The most accepted one is the carbide-mechanism, chain growth via $–CH_2-$ insertion into a growing chain, Figure (2.3.1). Carbon monoxide is adsorbed dissociatively then hydrogenated (hydrogen assisted dissociation). In enol mechanism chain growth is preceded through CO adsorption and then reaction with adsorbed hydrogen to form HCOH as the monomer unit. In the CO insertion mechanism chain growth is through CO insertion in a metal-alkyl bond and then hydrogenated to form alcohol or alkene [15]. In the case of alkyl mechanism, initiation is through elements from carbide and CO insertion, CO is converted to

surface carbide and the chain growth through insertion of alkenyl groups instead of alky groups.

2.4 Catalyst properties and C_{5+} selectivity

The selectivity is influenced by the support properties such as surface area, pore volume, pore size distribution and pore diameter as well as cobalt particle size. These effects are studied in earlier work [16][17].

The support's porosity and cobalt particle size have a significant effect on catalyst performance. The pore size of the support affects the Co_3O_4 crystallite diameter, catalyst reducibility and F-T synthesis activity. A large Co_3O_4 crystallite is enhanced when the pore size is large. The number of cobalt active sites on the catalyst surface then decreased and decreased the reducibility and furthermore the F-T activity is decreased [18]. Metal dispersion is in relation with cobalt particle size, as the Co_3O_4 particle size increases the dispersion decreases [27], see figure (2.4.1a)

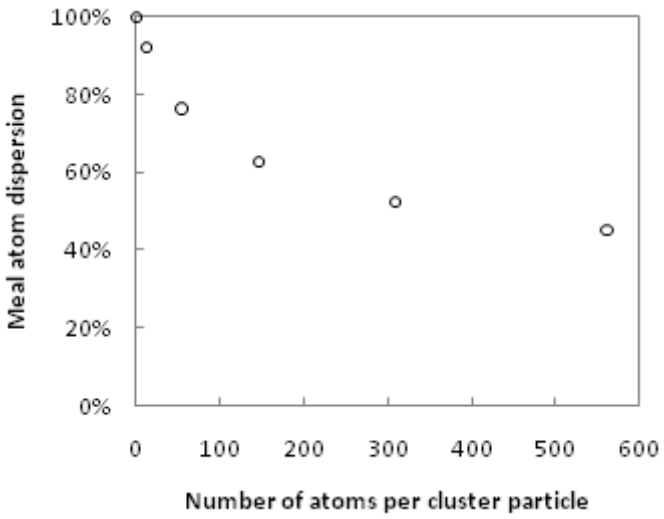

Figure 2.4.1a Metal dispersion vs partic 1

According to Iglesia et al. [19] the chain growth is a result of readsorption of α-olefins and the α-olefins are reactive as they are adsorbed into the growing chain and the readsorption of α-olefins depends on residence time in the supports pores and hence it was concluded that the supports nature had no contribution to the C_{5+} selectivity. The selectivity depends on a structural parameter, χ, which is an indication to intraparticle diffusion resistance [19] .

$$\chi = R_0^2 \, \varepsilon \, \Theta_{Co} / r_p$$

This parameter is a function of catalyst pellet size (R_0), porosity (ε), density of Co sites per unit area (Θ_{Co}), and pore radius (r_p). The optimum value C_{5+} selectivity was found for a χ between 500-1000.10^{16}. Figure (2.4.1b). This optimum is due to maximize the secondary chain building reactions. An increased secondary chain building reactions are increased by increasing intraparticle diffusion without inducing diffusion resistance to the reactants [19] which is a function of catalyst pellet size (R_0), porosity (ε), density of Co sites per unit area (Θ_{Co}), and pore radius (r_p). The optimum value C_{5+} selectivity was found for a χ between 500-1000.10^{16}.

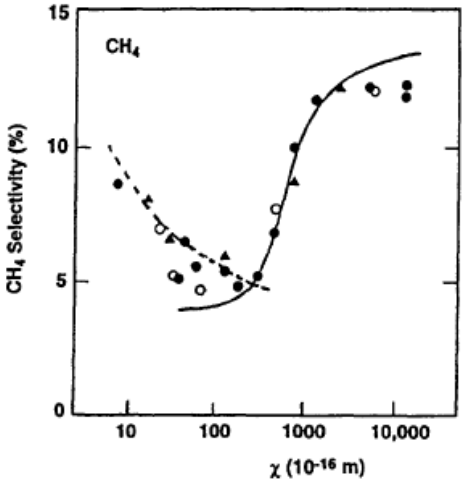

Figure 2.4.1b Effect of χ on F-T synthesis selectivity [12]

Any change caused by the olefin diffusion phenomen on C_{5+} selectivity for Co-Re catalysts supported in alumina was excluded by studying Co-Re γ and α- supported Al_2O_3 catalyst according to Rytter et al. and it was repported that the selectivity is influenced by catalyst particle size.Three catalysts were tested as shown in figure figure.(2.4.2a). CAT1,CAT2 and were γ-Al_2O_3 supported with pore diameters 7,3 and 15,5 nm while CAT3 was α-Al_2O_3 supported with pore diameter 200 nm.

The C_3 olefin to paraffin (O/P) ration was found as function of catalyst particle size. The C_3 olefin to paraffin ration decreased with increasing particle size at 45 and 10 % CO conversion. (Figure 2.4.2b) [20].

The C_3 olefin to paraffin ration decreased with increasing particle size at 45 and 10 % CO conversion. According to Borg et al. the C5+ selectivity was higher for wide pore suppoprt for γ-Al_2O_3 and some other supported catalysts.Figure (2.4.3) [13].

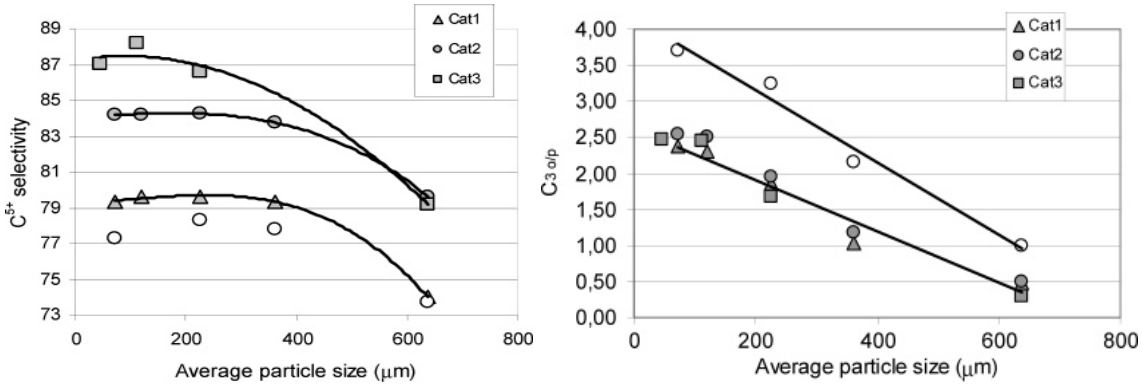

a b

Figure 2.4.2 a: C_{5+} selectivity vs catalyst particle size; b: C_3 O/P ratio vs catalyst particle size [23].

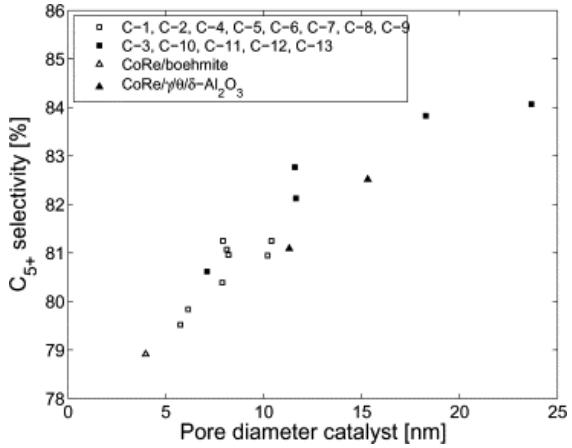

Figure 2.4.3 Relation between supports pore diameter and C5+ selectivity [13]

2.5 Catalyst deactivation

Deactivation is a phenomenon that appears with time in Fischer-Tropsch synthesis. There are some mechanism prposed for deactivation including: oxidation, sintering and solid state reactions leading to inactive cobalt. The deactivation due to sintering is more especially when the metal-support interaction is weak [14]**.** The Re-promoted catalysts deactivate more rapidly than the unpromoted catalysts. The CO conversion decreases with time on stream and as a consequence the C5+ selectivity drops.

Chapter 3

3.1 Alumina Support preparation

All alumina supports can be prepared from the parent γ-Al_2O_3 phase by heat treatment. In order to prepare the desired alumina phases, the γ-Al_2O_3 was heated up from 1023 K to subsequent higher temperature. Three different alumina phases (Medium pore) α , Θ and δ -Al_2O_3 were prepared by heating up to 1423,1323 and 1173 K respectively in flowing air and held in these temperatures for 10 hours. The heating rate was 10 K/ min up to 950 K and 1 K/min up to the final temperatures.

Afte heat treatment the alumina phases were investigated by X-ray diffraction to verify the phase.

3.2 Catalyst preparation

All catalysts were prepared by the method of one-step incipient wetness impregnation of alumina supports with cobalt nitrate hexahydrate, $Co(NO_3)_2.6H_2O$, perrhenic acid $HReO_4$ and dihydrogen hexa chloroplatinite acid H_2PtCl_6 as cobalt, rhenium and platinum precursors respectively. It must be mentioned that the platinum precursor was recommended by the supervisor where tetramine platinum nitrate could be used.

Prior to impregnation , the water absorption capacites of the alumina supports were determined by adding deionised water to the supports until they became saturated with water and appeared to be slyrry like and sticky. In this step no free flowing water observed.[14]. In the preparation of the catalysts the cobalt, rhenium and platinum loading was 12 ,0.5 and 0.5 % respectively. After evaluating the water absorption capacity the impregnation solution containg cobalt nitrate hexahydrate and perrhenic acid or dihydrogen hexachloroplatinite were mixed with alumina supports to form homogeneous mixture with no distinct phases present. These mixtures were then placed in a furnace and stirred after every 15 min and dried at 383 K. the drying time was 4 hours.

The dried samples were sieved both before and after calcination to remove catalyst particles smaller then 53 nm and larger then 90 nm. The calcination step was carried out in flowing air in a quartz reactor at 4 bar pressure and 573 K for 16 h. A heating rate of 2 K/min was used to heat up the samples to 573 K.

3.3 Support and catalyst characterisation

3.3.1 X-ray diffraction

X-ray diffraction patterns were recorded for all supports and catalysts on a Bruker AXS D8 focus diffractometer using CuKα radiation. All the samples were crushed prior to X-ray diffraction to produce fine particles. Table (3.1) shows the parameteres used in Xray diffraction.

Table 3.1 X-ray diffraction parameters [14]

Sample	2Θ° range	Step size(°)	Stepperiod(s)
Al_2O_3	15-75	0.04	7
Catalyst	32-43	0.04	8

The average Co_3O_4 crystallite thickness was calculated applying the Scherrer equation on the (311) diffraction peak located at 2Θ= 36.9°.

$$t = \frac{K\lambda}{\beta \cos\theta} \qquad (3.3.1)$$

$$\beta = \sqrt{B^2 - b^2} \qquad (3.3.2)$$

Where

t= Co3O4 crystallite thickness in nm

K= shape factor (0.89)

B= full with half maximum (FWHM) of Co_3O_4 peak at 2θ= 36.9°

b= instrumental width of the LaB_6 peak at 2θ= 35.5°

λ = wave length

Average spherical Co_3O_4 particle size is obtained by multiplying the crystallite thickness (t) by a factor of 4/3..

3.3.2 Hydrogen chemisorption

Hydrogen chemisorption as a standard technique to determind cobalt metal dispersion was performed on a Micromeritic ASAP 2010C figure (3.1). the catalyst sample was loaded into a U-shaped quartz reactor and place inside an electric furnace.A thermocouple placed outside the reactor controlled the temperature of the catalyst bed. Taks in H_2 chemisorption are presented in table (3.2). An adsorption isotherm was produced based on the amount of the hydrogen chemisorbed on the catalyst at different pressures ranging from 20 to 510mm Hg at

313 K. Metal dispersion (D%) is evaluated considering amount of hydrogen chemisorbed on the catalyst by extrapolating the straight line portion of the isotherm to zero pressure. In order to calculate the cobalt disperion it was assumed that one hydrogen molecule covers two cobalt sites and rhenium does not adsorb any hydrogen.[4].

Table 3.2 Tasks in H_2-chemisorption

Task No.	Task	Gas	Temperature K	Ramp rate K/min	Time min
1	Evacuate	Air	313	10	60
2	Evacuate	-	313	10	60
3	Leak	-	313	10	-
4	Flow	H_2	623	1	600
5	Evacuate	-	603	10	60
6	Evacuate	-	373	10	-
7	Leak	-	373	10	-
8	Analysis	H_2	313	10	-

A typical adsorption isotherm is shown in figure (3.2)

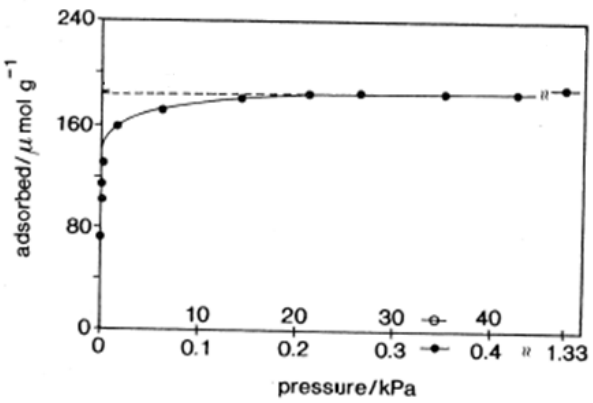

Figure 3.1 Typical H_2-chemisorption

The metal dispersion (D%) of the catalyst is calculated by using the following equation

$$D\% = \frac{V_{ads} \times f}{(wt_{Co} / W_{Co^\circ}) \times 22400} \qquad (3.3.3)$$

Where

V_{ads} = volume of hydrogen adsorbed in cm_3/g STP

D% = Co metal dispersion

wt_{Co} = wt.% of cobalt

W_{Co° = atomic weight of cobalt

f = stoichiometric factor = 2

The cobalt metal particle size is then calculated from the cobalt metal dispersion considering spherical, uniform cobalt metal particles with site density equal to 14.6/nm^2 [22].

$$D\% = \frac{f \times W_{Co^\circ}}{\rho \times A_{Co} \times N_A} \frac{S}{V} \qquad (3.3.4)$$

where

f = surface fraction of active phase=1

W_{Co° = 58.9 g/mol

A_{Co} = Area of cross section of cobalt atom = 0.66nm_2

N_A = Avogadro's number = $6.023.10^{23}$

ρ = density of cobalt = 8.9 g/cm^3

$\frac{S}{V}$ = surface to volume ratio

The following formula was deduced based on the above values:

$$d_{Co^\circ} = \frac{96}{D\%} nm \qquad (3.3.5)$$

The cobalt metallic surface area per gram of sample is the total active metal surface area available for interaction with adsorbate. The actual cobalt particle size is calculated by multiplying the degree of reduction based on oxygen titration.

$$S_{Co^\circ} = \frac{6.023 \times 10^{23}}{22400 \times wt_{Co^\circ}} \times V_{ds} \times f \times A_{Co} \qquad (3.3.6)$$

where

S_{Co° = Metallic surface area, m^2/g

V = Volume adsorbed (from analysis), cm^3/g STP

A = Effective area of 1 active metal atom, m^2/atom

f = Stoichiometry factor (2 for H_2, 1 for CO).

3.3.3 Temperature programmed reduction

The reducibility of the catalyst is evaluated by temperature programmed reduction (TPR). The catalysts samples of (0.2750g) were loaded into a U-shaped quartz reactor and heated up 1203 K in a flowing stream of 7%H_2 in Ar that was passed theough the reactor and the hydrogen consumption was measured. The heating rate was 10 K/min. Water and condensable product gases was removed by using a cold trap containing dry ice and liquid 2-propanol. The thermal conductivity detector (TCD) signal was analyzed by Shimadzu GC-8A gas chromatography instrument. The TPR set up is shown in picture (Show the picture here). A set up of TPR instrument is presented in figure(3.2).

3.4 Fischer-Tropsch synthesis

Fisher-Tropsch synthesis was performed in a reactor system which consists of two parallel fixed bed stainless steel reactors. An illustration of Fischer-Tropsch synthesis setup is given in figure (3.5).

A uniform temperature distribution along the catalyst is of great importance and for this purpose the samples were diluted with inert silicon carbide (SiC). Each sample contains 1.7 g catalyst containing 12% cobalt were mixed with silicon carbide.

Both reactors were pressurized by He gas upto 20 bar to check for any possible leakage. The pressure drop was then recorded after 15 h. The *in situ* reduction of the samples as a part of the procedure was performed in H_2 gas at 1 bar and at 623 K for 16 h while the temperature was increased by 1K/ min. After the reduction the samples were then cooled to 443 K. The pressure in both reactors was increased to 20 bar and the synthesis gas of molar ration H_2/CO = 2.1 was introduced into the reactors and the temperature was raised slowly to 483 K to avoid runaway and possible catalyst deactivation.

The experiment consists of two periods:

1^{st} period: Synthesis gas (250 ml/min) to be introduced and maintained at this condition for 24 h.

2^{nd} period: The synthesis gas flow to be adjusted to give an initial CO conversion of 50%.

Heavy hydrocarbons are collected in a hot trap (358-363 K) and other liquid products are collected in a cold trap (298 K). The product gas mixtures (CO, N_2, H_2, CO_2 and C1-C9) are

to be analyzed with an on-line GC equipped with thermal conductivity (TC) and flame ionization (FI) detectors.

Co reaction rate and turnover frequencies were obtained. The turnover frequency based on hydrogen chemisorption data is calculated from:

$$TOF_{H2=} = -r_{CO}.M_{Co}/(D_{Co}.X_{Co}) \quad (3.3.7)$$

Where

r_{CO} is the reaction rate for CO
M_{Co} is the molar weight of cobalt
D_{Co} is cobalt dispersion (here the dispersion is for Co-Pt/ Θ-alumina1)
X_{Co} is cobalt fraction in the catalyst.

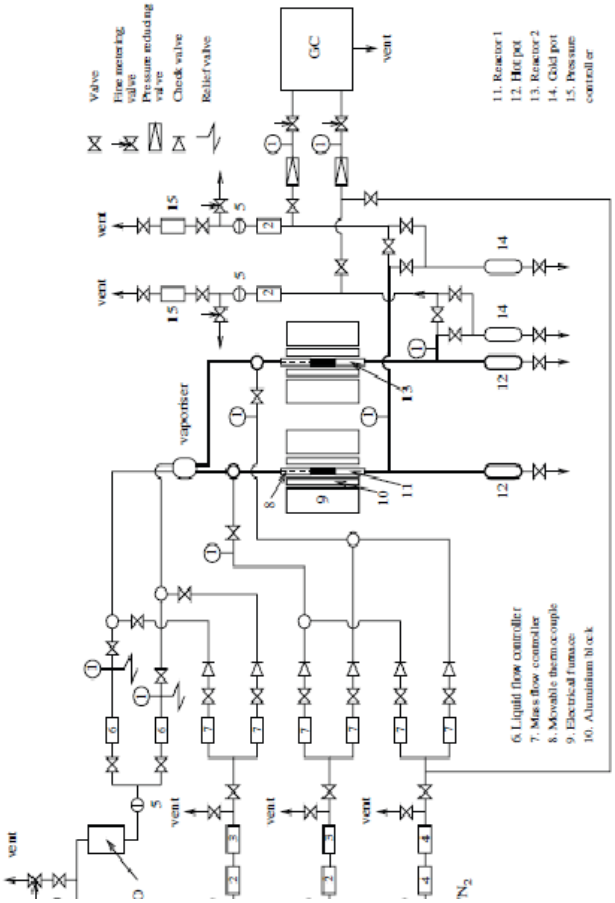

Figure 3.5: Fischer-Tropsch synthesis set up

3.4 Health, Environment and Safety (HES)

As indicated in the NTNU goals of Health, Environment and Safety, the work and learning environment must support and promote its users' capacity to work and learn, safeguard their

health and well-being, and protect them against work-related illnesses and accidents. HES-related problems should be solved consecutively at the lowest possible level, in order to prevent employees or students from developing work-related illnesses or suffering work-related accidents, and to prevent the activities from having a negative impact on the environment.

Risk assessment is an important tool for a chemical process operation which is the determination of quantitative or qualitative value of risk related to a concrete situation and a recognized hazard. A risk assessment must be carried out prior to the commencement of a specified chemical process and again when the process is modified. This risk assessment is done to remove or control the risk factors during the operational period of the chemical process.

The activities associated with several HES issues on the F-T synthesis set-up are:

- Handling of hazardous chemicals
- Modification and maintained of experimental set-up
- Transport and mounting of the gas bottle
- Catalyst Synthesis
- Handling of the catalyst

For existing risk assessments, safety measures, rules and procedures are as follows:

- In the F-T synthesis set-up, a well-established toxic and flammable gas alarm system exists. So in the case of leak, the gas alarm system will able to inform and necessary action concerning the HES can be taken according to rules and procedure.
- For personal protection, safety goggle is very important in labs and it is mandatory for everyone who is working inside the lab.
- Leak test is an important procedure for decreasing the risks related to the toxic and combustible gases.

The HES assessment identification processes, risk assessment, HES action plane for F-T synthesis set-up are shown in appendix (A).

The main risk concerning with toxic and combustible gases

Risk concerning with carbon monoxide: Carbon monoxide is a colorless and odorless gas; it comes as synthesis gas component for DME synthesis. The chemical company YARA PRAXAIR is supplier of synthesis gas in our lab. Carbon monoxide is extremely flammable

and toxic. It may cause harm to the unborn child and danger of serious damage to health by prolonged exposure through inhalation. This gas should be keeping away from the source of ignition and should be store in safe area as the condition of flammable gas storage. It needs to use in well-ventilated area and in case of fire, this gas should be allowed to burn if flow cannot be shut off immediately and need to immediate contact responsible person.

Risk concerning with Hydrogen: Hydrogen is a colorless and odorless gas and extremely flammable gas, stable under recommended storage and condition. Inhalation of vapor may cause dizziness, an irregular heartbeat, narcosis, nausea or asphyxiation. If anyone inhaled, remove to fresh air. This substance classified with a health or environmental hazard. This gas should be disposed as hazardous waste. This gas should be keeping away from the source of ignition. Personal protection is necessary like goggles, apron, vent hood and protective gloves in used area and it needs to use in well-ventilated area [24].

4. Results and discussions

In objective of this project is to explore the the effect of promoters (Pt,Re) on the catalystic performance(i.e activity). The first part of this project deals with the characterisation of the catalyst Different alumina phases α,Θ, δ and γ -Al_2O_3 were prepared from the parent alumina phase namely γ-Al_2O_3 samples by heat treatment and the second part deals with testing of the catalysts performance. It is important to mention that due to a mistake in calculation, the weight% of the metal promoters (Pt,Re) is higher than 0.5% and is approximately around 1.1 and 0.7wt % respectively. Later two other samples were prepared with correct cobalt and platinum loading. These two samples were Co-Pt/α-Al_2O_3 and Co-Pt/Θ- Al_2O_3.

The temperatures at which thses alumina phases were formed are shown in figure (4.1).

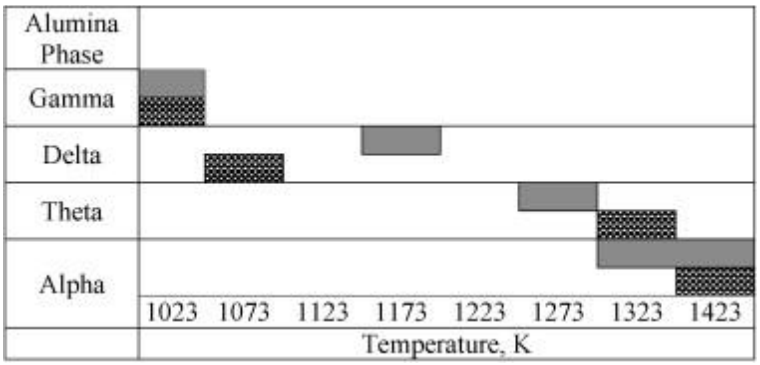

Figure 4.1 Heating temperatures for different alumina phases

4.1 X-ray diffraction

The alumina phases were identified by X-ray diffraction as shown in figure (4.1.1). The crystallite thickness of each alumina sample was calculated by fitting the diffraction data using Bruker Topas v4.2 software. The X-ray diffraction patterns for all alumina phases and catalysts are given in figure (4.1.1 a) and figure (4.1.1 b) respectively.

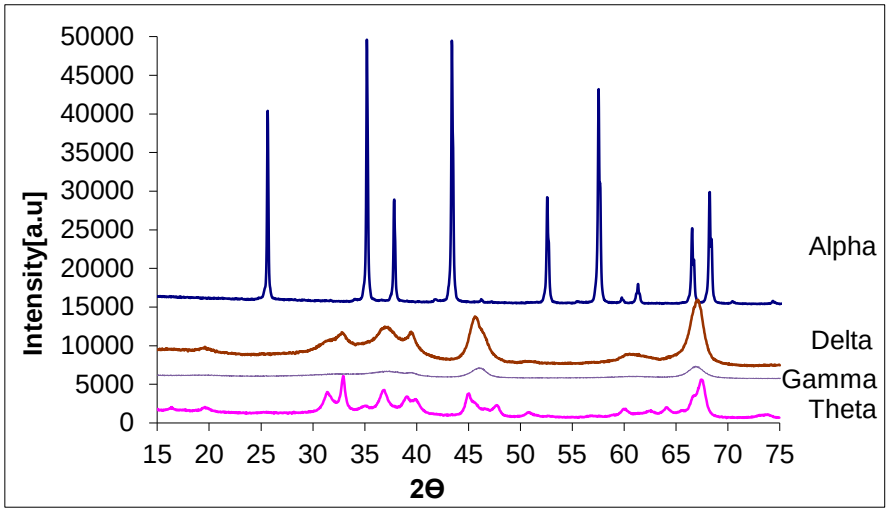

Figure 4.1.1a:X-ray diffraction patterns for alumina phases

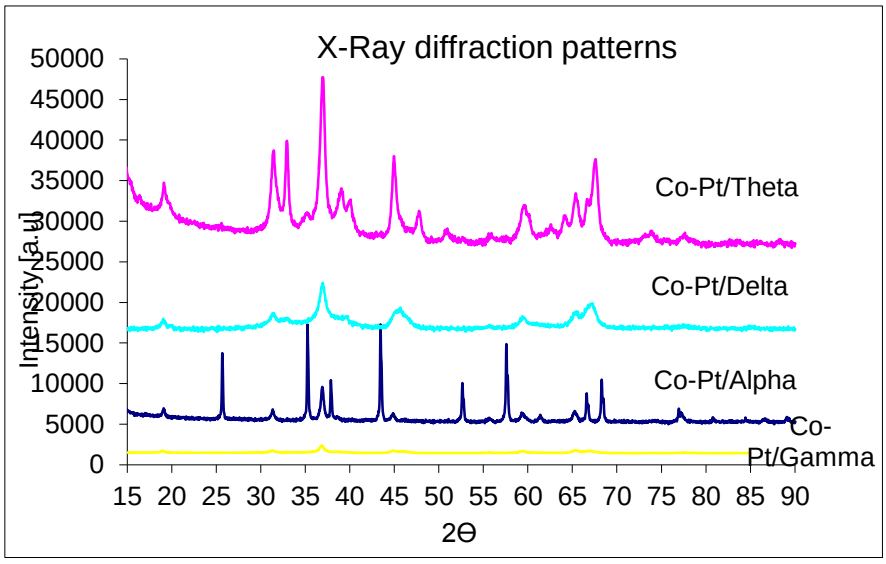

Figure 4.1.1b: X-ray diffraction pattern for all catalysts

The characterisation results of alumina supports are presented in table (4.1.1)

Table 4.1.1 Characterization results of alumina samples

Sample	Alumina support	Crystallite size of alumina (nm)
MP-1423	Alpha	88,7
MP-1323	Theta	10,7
MP-1173	Delta	9,2
MP-1023	Gamma	5,3

MP-1423 denotes ‘Medium pore’ and the heating temperature for alumina

Totally six samples of catalysts were prepared by the method of incipient wetness impregnation. Two samples with 12 and 0.7 wt% cobalt and rhenium loading respectively and four samples with 12 and 1.1 wt% cobalt and platinum loading respectively on differnet alumina supports. The catalyst samples were investigated by X-ray diffraction and the diffraction data was in 2Θ° the range of 15° to 85° and Co_3O_4 cryatallite thickness was calculated for all catalyst samples. The results are to be found in table (4.1.2).The metal dispersion is low for all Pt-promoted catalysts and for Re-promoted alpha alumina supported catalyst .on since the Co_3O_4 are large and this relation between metal dispersion and particle size was illustrated in figure (4.1.1a).

Table 4.1.2 results of Co_3O_4 and cobalt particle size for MP catalysts

X-Ray diffraction			H_2-chemisorption		
Catalyst	Co_3O_4 particle size(nm)	Cobalt particle size#,(nm)	Cobalt particle size(nm)	Cobalt metal dispersion (D %)	
				Run 1	Run 2
Co-Re/Alpha	43.7	32,77	(40,4)	2.5	-
Co-Re/Theta	11.2	8,4	(13)	7.6	-
Co-Pt/Alpha	27.3	20,47	(60)	1.2	1.6
Co-Pt/Theta1	13.7	10,27	(41.9)	2.4	-
Co-Pt/Theta2	13.7	10.27	(29)	3.38	-
Co-Pt/Delta	8.7	6,52	(47.5)	2.1	-
CoPt/Gamma	12.6	9,53	(29)	3.5	-

#d_{Co} = 0.75(dCo_3O_4)nm

4.2 Temperature Programmed reduction

The reducibility of the catalyst samples was studied by Temperature programmed reduction (TPR) and their profiles are shown in figure (4.2.1a). The addition of promoter to the catalysts affects the reducibility of the catalysts positively where the cobalt oxides are reduced to metallic Co.[29]. The reduction peaks are shifted to a lower reduction temperature presumably due to the hydrogen spillover to the cobalt oxides.[30]. The promotion with noble metals (Pt here) increases the number if cobalt surface sites and reduces the interaction

between the small surface species and the support. A comparison of monometallic catalysts [14] and bimetallic (promoted) catalysts is shown in figure (4.2.1b). The addition of noble metal promoters is believed to affect cobalt nitrate decomposition and improves cobalt dispersion. [28]

The reduction of cobalt oxide Co_3O_4 involves two steps with an intermdiate CoO formation which is furthere reduced to Co in the second step [14]. The first step represents the reduction of Co_3O_4 to CoO and the second step is assigned to the reduction of CoO to Co. In the TPR profiles most of the catalysts exhibit three peaks. The first peak is attributed to decomposition of residual cobalt nitrate remaining after calcination step which indicates that the calcination temperature was not high enough to decompose all the cobalt nitrate.[33]. The second peak (low temperature peak) is attributed to the reduction of Co_3O_4 to CoO and the third peak to the reduction of CoO to metallic cobalt (Co). The adjucent temperatures are shown on the peaks.

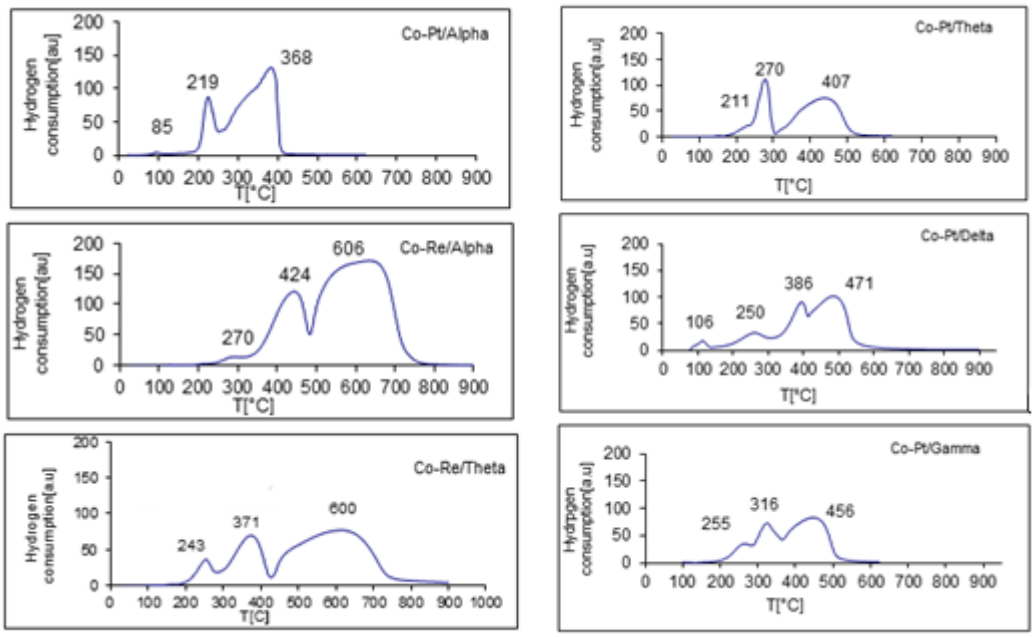

Figure4.2.1a: TPR profiles of Re and Pt-promoted cobalt catalysts

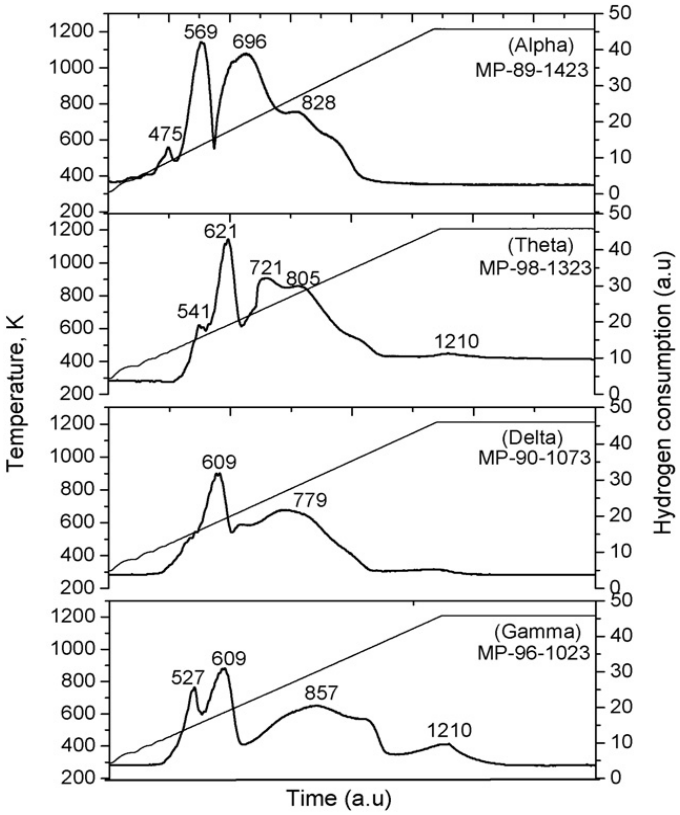

Figure 4.2.1b: TPR profiles of unpromote cobalt catalysts. [14]

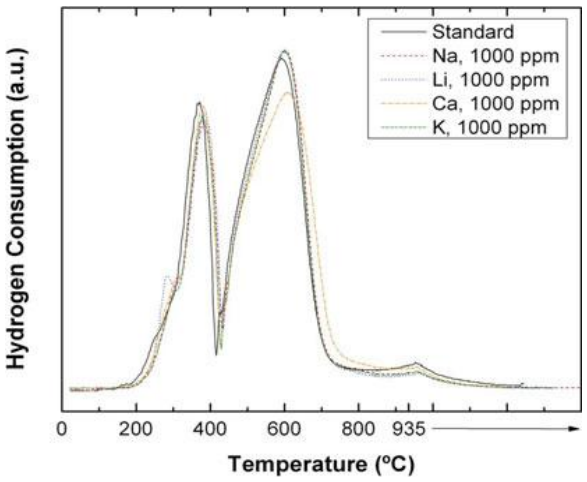

Figure 4.2.1c: TPR profiles for Co-Re/ γ-alumina. [41]

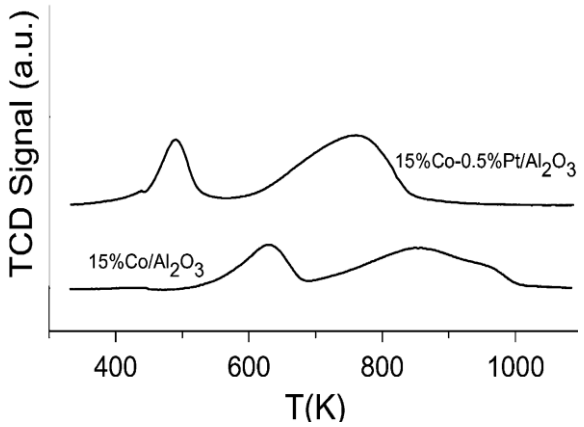

Figure 4.2.1d: TPR profiles of promoted and unpromoted cobalt catalysts. [31]

Furthermore two extra TPR profile for both unpromoted and promoted cobalt catalyst is shown in figure (4.2.1c) [41] and figure (4.2.1d) [31].

During the Temperature Programmed Reduction process, not all catalyst samples were heated up to 900 °C as it is clear from the TPR profiles. This is because there was not found any reduction peaks above 600°C for promoted cobalt catalysts in literature. The following samples Co-Pt/α-alumina, Co-Pt/Θ-alumina, Co-Pt/δ-alumina and Co-Pt/γ-alumina were heated up to 600°C. In contrast to the TPR profiles of unpromoted catalysts in figure (4.2.1b) no peaks were found above 500°C for samples mentioned previously and this may indicate that a low concentration of bulk barely reducible in the catalysts. [32].

First peak for all catalysta in figure (4.2.1a) except the catalyst Co-Pt/ δ-alumina indicates the decomposition of residual cobalt nitrate remaining after calcination. The first peak for Co-Pt/ δ-alumina is probably due to unstable signal at the start. A comparson between TPR profiles in figures (4.2.1a) and (4.2.1b) shows that reduction peaks for promoted catalysts appear at lower reduction temperature.The second peak for Co-Pt/ α-alumina appears around 219-220 °C which is lower compared to 293 °C for the unpromoted Co/ α-alumina in figure (4.2.1b). The third peak appears at 368 °C which is much lower than 423 °C for the unpromoted catalyst. The presence of doublet and shoulder in both Co-Pt/ α-alumina and Co-Pt/ δ-alumina catalysts is due to the presence of NO_3^- species according to Khodakov [32].

The first, second and thirs peaks at 211,270 and 407 °C for Co-Pt/ Θ-alumina sample against 268,348 and 448 °C for Co/ Θ-alumina in figure (4.2.1b) show how the addition of promoter affects the reduction temperatures. There is even a fourth peak at 555 °C that may be an indication of bulk cobalt species thar are reduced at high temperature. A lower reduction temperature is observed for all other Co-Pt/alumina in figure (4.2.1a) catalysts compared to unpromoted catalysts. According to Wenping et al. [35] the Pt- oxides are reduced at lower

temperature than Re-oxides, and in the case of Co-Pt/ α-alumina the peaks appear at temperature lower than peaks in Co-Re/ α-alumina in figure (4.2.1a).

Balonek et al.[41] investigated the effect of alkali metal impurities on Co-Re catalysts. Although the cobalt loading is higher (20 wt%) and the support is gamma alumina, a comparson between the standard catalyst in figure (4.2.1c) and Co-Re/ α-alumina or Co-Re/ Θ-alumina in figure (4.2.1a) shows that the first reduction peak in figure (4.2.1c) occurs at 372 °C and the second reduction peak at 589 °C which is close to reduction temperatures (424 °C, 606 °C) and (371°C, 600°C) for Co-Re/ α-alumina and Co-Re/ Θ-alumina respectively in figure (4.2.1a). In figure (4.2.1d) the low temperature peak appears approximately at 220 °C compared to 316 °C in figure (4.2.1a) and highe temperature peak appears approximately at 477 °C compared to 456 °C which is lower. An increase in cobalt loading increases average cluster size and therfore results in higher percentage reduction and reduction occurs at lower temperature than catalysts in figure (4.2.1a).[31]. As mentioned previously, the presence of chlorine may affect the reduction temperature due to surface coverage by chlorine which will be covered later in chapterr (4.3).

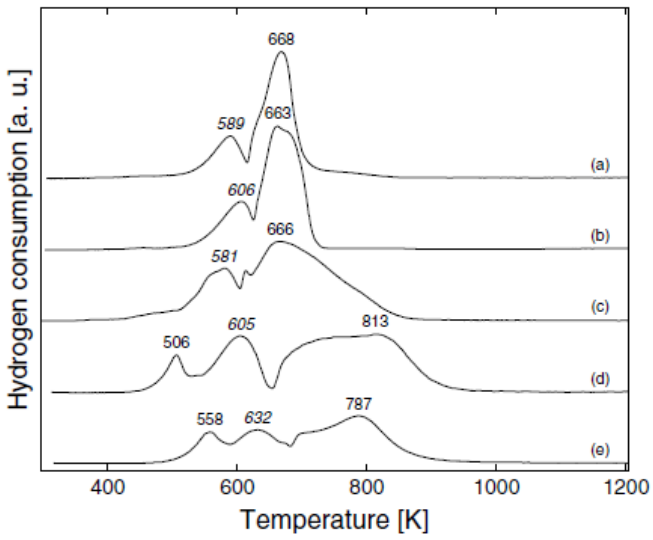

Figure4.2.1e: TPR profiles of 20Co-Re/α -Al_2O_3(c), 20Co-Re/ γ -Al_2O_3(d), 12Co-Re/ γ -Al_2O_3(e) [4]

Figure (4.2.1e) shows TPR profiles for Co-Re/ α-alumina and Co-Re/ γ-alumina with different cobalt loading taken from Ø. Borg Theses [4]. The low and higher temperature peaks for catalyats in figure (4.2.1d) appear at lower temperature than reduction peaks in figure (5.2.1a). 20Co-Re/α -Al_2O_3(c) has higher cobalt loading and this could reduce the reduction temperature. However the difference in temperature is quite big something that is difficult to explain. The second and third peaks appear at 424 °C and 606°C respectively for

12Co-Re/α -Al_2O_3 catalyst in figure (4.2.1a) but these peaks appear at 308 and 393°C for 20Co-Re/α -Al_2O_3 in figure (4.2.1d). Another TPR profile taken from Enger et al. [39] is shown in figure (4.2.1f).

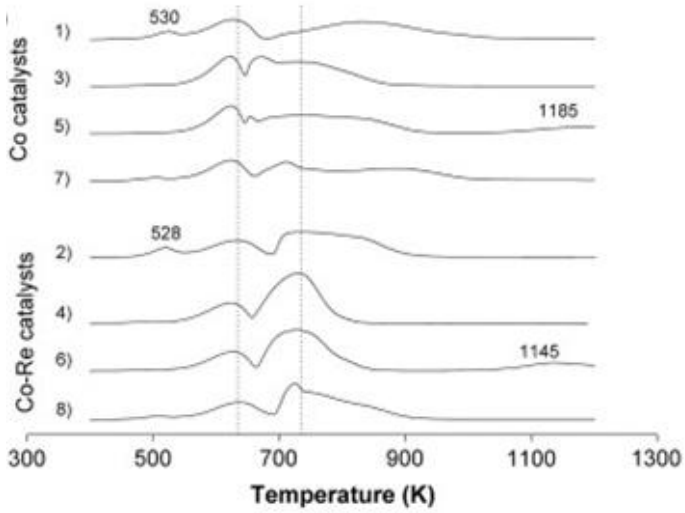

Figure 4.2.1f: Temperature-programmed reduction for 12 wt% Co (+0.5 wt% Re) over α -Al_2O_3 profile number 4)

The TPR profile (3) which is for 12%Co-Re/ α -Al_2O_3 exhibits higher reduction temperature (362 and 462°C) which is higher than those in Borg et al. even though the Co3O4 particle size is close to the particle size in Borg et al

4.3 Hydrogen chemisorption

The catalyist activity is improved with enhanced cobalt dispersion. According to Schanke et al.[36] Pt- promotion increased the cobalt dispersion. The cobalt metal dispersion was calculated by H_2-chemisorption. Diehl et al.[37] does not recommend precursors that contain halides [$RuCl_3$ or H_2PtCl_6] as noblemetall precursors. This is probably because of the modification effect of such precursors on the cobalt catalyst and in addition halides are poison for cobalt catalysts. Theses modification could affect the structure of the cobalt catalyst, the reducibility of cobalt, the cobalt dispersion and formation of barely reducible cobalt support compounds. [37]. Borg et al. [38] invistigated the reduction of cobalt surface in presence of chlorine. The chlorine covers the cobalt surface and this limits the hydrogen uptake. Since cobalt dispersion is calculated based on hydrogen uptake, the surface coverage affect the cobalt dispersion. This could be an explanation for the low dispersion observed in all Pt-promoted cobalt catalysts. The result of H_2 chemisorption is presented in table (4.1.1). The lowest dispersion is for α-alumina du to large Co_3O_4 particles. Isotherms for catalyst samples are presented in (Appendice C).

The lowest dispersion was observed for both Co-Re/ Pt promoted α -Al_2O_3. The low surface area of α -Al_2O_3 may be a reason for low dispersion.

It is of importance to mention that in this work no ethylene glycol was used to controll the ceystallite thickness of Co_3O_4 and the Co_3O_4 crystallites are large compared to those in Shreya's theses.[14] and the dispersion would be lower for large Co_3O_4 crystallites [12].
In the preparation of the alumina phases by heat treatment a deviation of 7-9 C° in temperature set point was observed as well as an overshoot when heating up samples.
In the characterization step by the method of X-ray diffraction, a large Co_3O_4 crystallite size vale was obtained.

4.4 Activity and selectivity

In this section the effect of metal promotion and promoter's precursor on the catalyst performance was investigated . The activity and selectivity of catalyst samples were studied . Since the dispersion was low for all platina promoted catalysts, it was recommended by the supervisor to test only two of the catalysts. Catlaysts Co-Pt/ α-alumina and Co-Pt/ Θ-alumina1 were chosen for this purpose. The activity for the catalyst Co-Pt/ α-alumina was measured and found to be too low to see any CO conversion. The activity of this catalyst is presented in figure (4.4.1). As it is shown the catalysts is almost inactive. This is due to the blocking of active cobalt sites by the chlorine that is present on cobalt atoms [38]. This makes the cobalt sites inaccessible for reaction. In this experiment no water was added to the reaction mixture. According to Borg et al. [12] a small of water would probably had a positive effect on CO conversion and starting the reaction in order to wash away the chlorine present on the cobalt surface. The selectivity is not presented here since the activity was too low.
The catalyst Co-Pt/ Θ-alumina1 activity is shown in figure (4.4.2). As shown in the figure the result is very interesting. The activity increases with time on stream even after 60 hours on stream. Borg et al. [38] assumed that the chlorine is removed from the cobalt surface under Fischer-Tropsch reaction. The increasing activity with time on stream could be explained by the removal of the chlorine from the cobalt surface according to Borg et al. Since the amount of chlorine is large, it takes time to remove the chlorine and the CO conversion increases as the chlorine is removed from the surface and furthermore more cobalt sites are accessible for

the reaction and hence higher activity is observed. Borg et al. [38] found negligible effect on activity and no effect on selectivity for modified catalyst with small amount of chlorine. A large amount of chlorine affects time on stream and makes it longer in order to reach a stable activity. During the chemisorption the condition is not sever enough to remove the chlorine as it is in Fischer-Tropsch reaction something which explains the low dispersion [38].

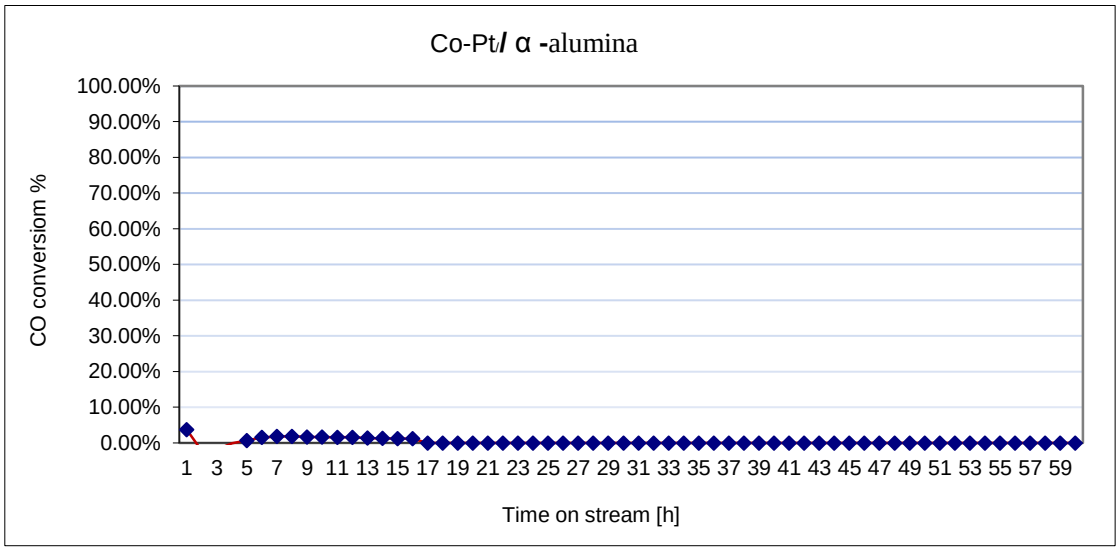

Figure 4.4.1: The conversion of CO as a function of time on stream for Co-Pt/ α-alumina catalyst

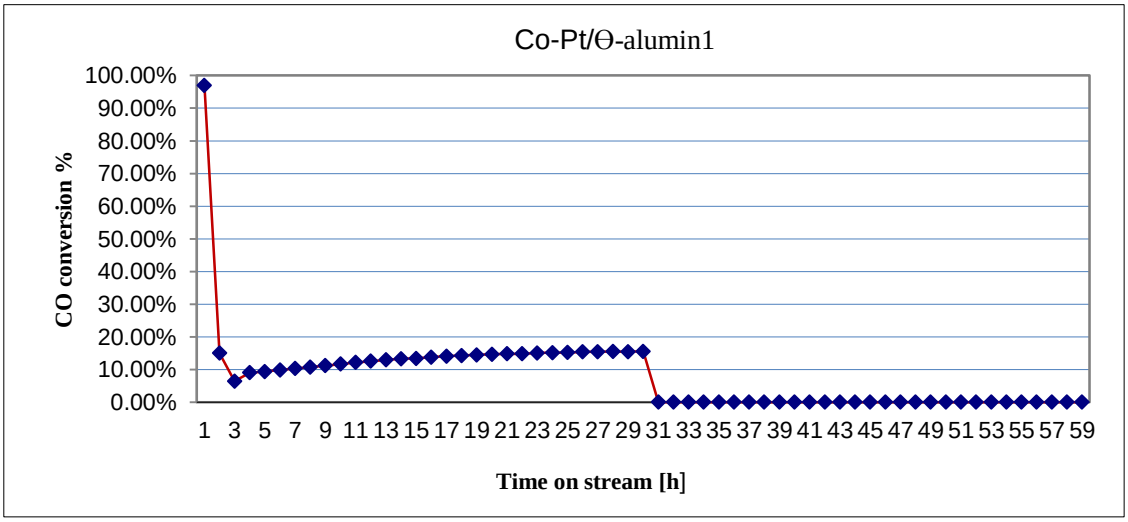

Figure 4.4.2: The conversion of CO as a function of time on stream for Co-Pt/ Θ-alumina catalyst

According to the data in figure (4.4.3) the selectivity increses as the CO conversion increases with time on stream. As a matter of fact the F-T reaction was stopped before the activity reaches a steady state or a stable phase because it was not clear how long it would take for the catalyst to reach a stable activity to increase the Co conversion.

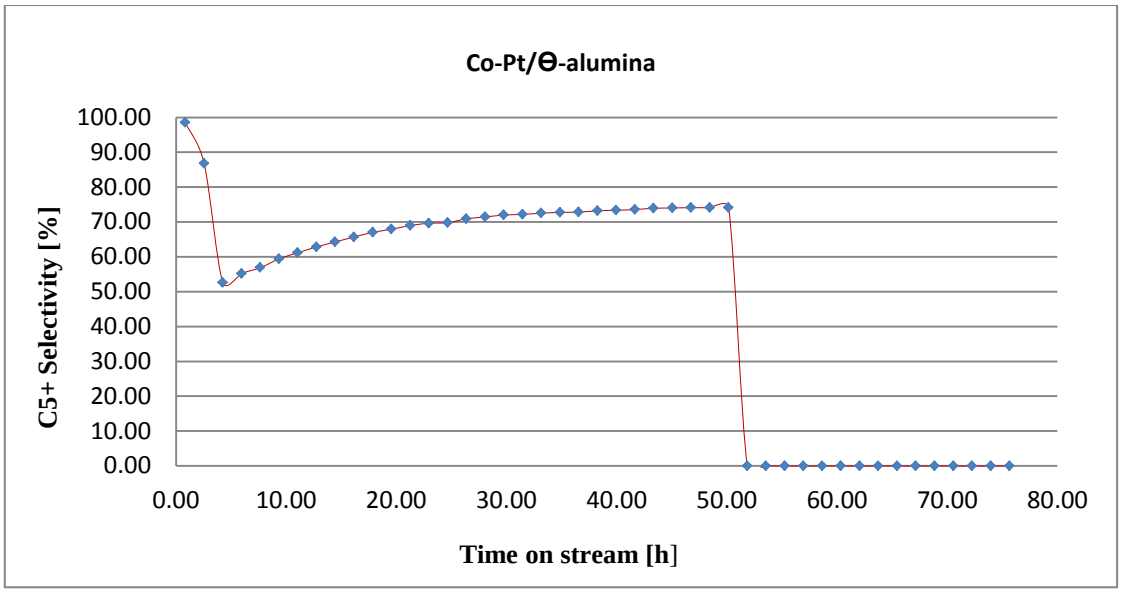

Figure 4.4.3: The selectivity as a function of time on stream for for Co-Pt/ Θ-alumina1 catalyst

In this section only the selectivity for Co-Pt/ Θ-alumina1 catalyst is presented in the figure above. The Co-Pt/ α-alumina was almost inactive due to law cobalt dispersion since the cobalt surface was covered by chlorine.

4.5 Turn over frequency

Turn over frequency for the Co-Pt/ Θ-alumina1 catalyst was calculated from the equation below:

$$TOF_{H2=} = -r_{CO}.M_{Co}/(D_{Co}.X_{Co})$$

The turn over frequency for Co-Pt/ Θ-alumina1 after 18 hours on stream was found to be 0,5710 (s^{-1}). The turn over frequency is high inspite of low dispersion because with time on stream the chlorine is removed from the surface and more cobalt surface is accessible.

4.5 Discussion

The metal promotion has measurable effect on the catalytic performance, reducibility and cobalt metal dispersion.

The most surprising effect of metal promotion is shifting the reduction temperatures to lower temperatures and hence more easily reduction of the cobalt oxide species. The metal promotion precursor was found to affect the catalytic performance where platinum precursors containing chlorine seems to lower the dispersion. The activity is also affected specially in the case of Co-Pt/ Ɵ- alumina where the surface are is higher compared to low surface area Co-Pt/ α - alumina catalyst and the activity increased with the removal of chlorine from the cobalt surface.

References

[1] Stat review of world energy 2000, http://www.BP.com.

[2] http://www.exxonmobil.com.

[3] World energy outlook 2011 special repport.

[4] Ø. Borg, *Roles of alumina support in Fischer-Tropsch Synthesis*, Doctoral thesis 2007

[5] Ber. Deut. Chem. Gesell., vol.30 1987 , pp.135-139; Chem. Zentralb.,1897,I,p.354; Jour.Chem.Soc.,1897,I,p.179.

[6] Hydrocarbon publishing company worldwide refinery processing review, third quarter.

[7] J. A. Moulijn, M. Makkee, and A. van Diepen. *Chemical process Technology*. John Wiley & sons, Ltd., Chichester, 2001.

[8] German patent 293, 787 'Process for production of hydrocarbons and their dericatives', assisted to BASF, granted March 8, 1913.

[9] http://www.altonaenergy.com/project_gasification.php.

[10] M.E.D Dry. High quality diesel via FT process-a review. *j. chem. Technol. Biotechnol*.,77:43-50,2001.

[11] I. Chorkendorff, J.W. Niemantsverdriet, *Concept of modern catalysis and kinetics*, WILEY-VCH verlag GmbH& Co,2003,p 193.

[12] Ø. Borg, S. Eri, E.A Blekkan, S. Storsæter, H. Wigum, E. Rytter, A. Holmen, *variables, FischerTropsch synthesis over γ alumina-supported cobalt catalysts: Effect of support Variables. J. Catal*. 248 (2007) .

[13] J. Zhang, J. chen, J. Ren, Y. Sun. *Chemical treatment of γ- Al_2O_3 and its influence on the properties of Co –based catalysts for Fischer-Tropsch synthesis. Appl. Catal. A*, 243121 2003.

[14] S. Rane, *Relation between Catalyst properties and selectivity in Fischer-Tropsch Synthesis. 2011.*

[15] B. Davis, Fischer-Tropsch synthesis: *Current mechanism and futuristic needs, Fuel Process Technol*. Catal. 26 (2003) 73.

[16] H. Xiong, Y. Zhang, S. Wang, J. Li, *Fischer-Tropsch synthesis: the effect of alumina porosity on the performance of Co/Al_2O_3 catalyst*. Catal. Comm. 6 (2006) 512.

[17] R. Bechara, D. Balloy, D. Vanhove, *Catalyst properties of Co/Al2O3 system for hydrocarbon synthesis*, Appl. Catal A 207 (2001) 343.

[18] R.C. Reuel, C.H Bartholomew, *The stoichiometries of H2 and CO adsorptions on cobalt: effect of support and preparation*, J.Catal.85(1984) 63.

[19] E. Iglesia, Design, *Synthesis and use of cobalt-based Fischer-Tropsch synthesis catalysts*, Appl. Catal. A 161 (1997) 59.

[20] D. Schanke, S. Eri, E. Rytter, C Aaserud, A. M Hilmen, O. A Lindvåg, E. Bergene, A. Holmen, *Fischer-Tropsch synthesis on cobalt catalysts supported on different Aluminas.*

[21] Erling Rytter, Sigrid Eri, Torild Hulsund Skagseth, Dag Schanke, Edvard Bergene Rune Myrstad, and Asbjørn Lindvåg, *Catalyst particle size of cobalt/rhenium on porous alumina and the effect on Fischer-Tropsch catalytic performance*, Ind. Chem. Res. 46 (2007) 9032.

[22] Ø. Borg, A. Holmen, *F-T synthesis over gamma alumina supported cobalt catalysts of support variables*, J. Catal. 248 (2007)89.

[23] Safety data sheet, Yara Praxair AS, Oslo, Norway

[24] Y. Ji, Z. Zhao, A. Duan, G. Jiang, J. Liu, *Comparativestudy on the formation and Reduction reduction of bulk and Al_2O_3-supported Cobalt oxides by H_2-TPR technique.* J. Phys. Chem. C. 113 (2009) 7186.

[25] www.statoil.com

[26] www.oed.no

[27] Martino, G (1979). "clusters: Models and precursors for metallic catalysts". *Growth and Properties of Metal Clusters*. Amsterdam: Elsevier Scientific Publishing Company. pp. 399–413

[28] J,-S. Girardon, A. Constant-Griboval, L. Gengembre,P.A. Chernavskii,A.Y. Khodakov, Catal. Today 106 (2005) 161.

[29] D. Shanke, S. Vada, S. Blekkan, E.A. Hilmen, A. Hoff and A. Holmen, J. Catal.156 (1995) 85.

[30] A. Hoff, PhD Thesis, University of Trondheim, Norway (1993).

[31] Gary Jacobs, Tapan K.Das, Youngqing, Jinlin , *Fischer-Tropsch synthesis support, loading and promoter effects on reducibility of cobalt catalysts.*

[32] Heline Karaca, Olga V. Safonova, Stephane Chambrey, Pascal Fongerlan, Anne G.Constant, A. Khodakov, *Structure and catalytic performance of Pt-promoted alumina supported cobalt catalysts under realistisc conditions of Fischer-Tropsch synthesis*.

[33] Ø. Borg, S. Eri, D.Akporiaye, B. Vigerust, E. Rytter, A. Holmen, Top. Catal. (2007), doi:10.1007/s11244-002007-0237-1.

[34] Wei Chu, Petr A. Chermavskii, Leon Gengembre, Galina A. Pankina, Pascal Fogerland, Andrei Y. Khodakov: *Cobalt species in promoted cobalt alumina-supported Fischer-Tropsch catalysts.*

[35] Wenping Ma, Gary Jacobs, Robert A. Keogh, Dragomir B. Bukur, Burtron H. Davis: *Fischer–Tropsch synthesis: Effect of Pd, Pt, Re, and Ru noble metal promoters on the activity and selectivity of a 25%Co/Al2O3 catalyst*

[35] G. Jacobs, T.K. Das, Y.Q. Zhang, J. Li, G. Racoillet, B.H. Davis, Appl. Catal. A: Gen. 233 (2002) 263–281.

[36] Schanke D., Vada S., Blekkan E.A., Hilmen A.M, Hoff A,Holmen A. (1995) *Study of Pt-Promoted Cobalt CO Hydrogenation.*Catalysts, *J. Catal.* **156**, 85-95; Vada S., Hoff A. Adnanes E, Schanke D, Holmen A. (1995) *Top. Catal.* **2**, 155-162.

[37] F. Diehl, A.Y. Khodakov: *Promotion of Cobalt Fischer-Tropsch Catalysts with Noble Metals: a Review*

[38] Øyvind Borg , Nina Hammer, Bjørn Christian Enger , Rune Myrstad , Odd Asbjørn Lindvåg , Sigrid Eri , Torild Hulsund Skagseth , Erling Rytter: *Effect of biomass-derived synthesis gas impurity elements on cobalt Fischer–Tropsch catalyst performance including in situ sulphur and nitrogen addition.*

[39] Bjørn Christian Enger, Åse-Lill Fossen, Øyvind Borg, Erling Rytter, Anders Holmen: *Modified alumina as catalyst support for cobalt in the Fischer–Tropsch synthesis*

[40] A. Y. Khodakov, J. Lynch, D. Bazin, B. Rebours, N. Zanier, B. Moisson, P. Chaumette, J. Catal. 168 (1997) 16.

[41] Christine M. Balonek , Andreas H. Lillebø , Shreyas Rane , Erling Rytter , Lanny D. Schmidt, Anders Holmen: *Effect of Alkali Metal Impurities on Co–Re Catalyst for Fischer–Tropsch Synthesis from Biomass-Derived Syngas*

Appendices

Appendice A

Gas warning system protects lives and health by monitoring the atmosphere inside the rig and triggering an optical and acoustic alarm, as soon as the concentration of the gas (**Hydrogen** and **Carbon monoxide**) that is being monitored exceeds the preset threshold level.Figure (A1).

Figure A1: Overview of the Gas warning system (External and Internal views)

When alarm starts, first of all we have to turn off the alarm. Secondly, solve the problem (Sometimes experiment has to be stopped). **Procedure for stopping the Gas warning system:**

Step 1 Shift the button to the right and wait for the **point (**for example **point 2-** Figur A2**).**

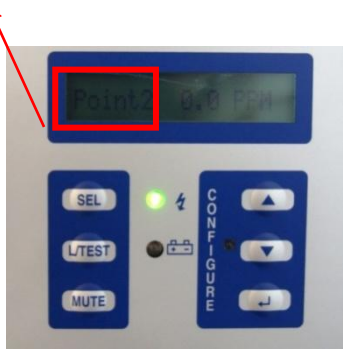

Figure A2: Gas alarm system monitor

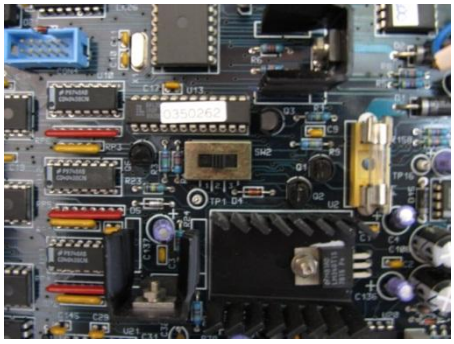

Figure A3: shift the button to the right

Step 2 Press **[SEL]**

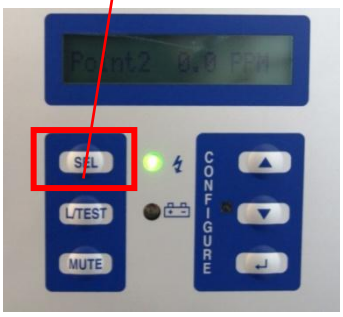

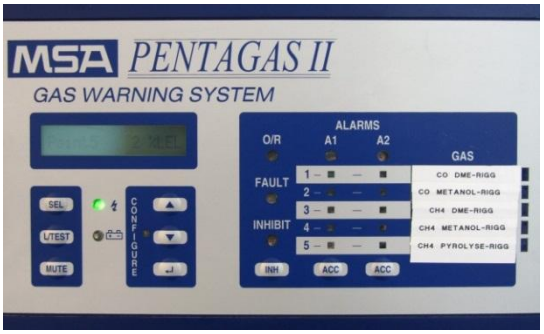

Step 3 Press **[INH]**

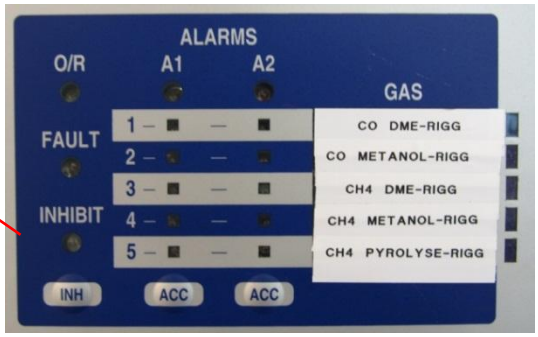

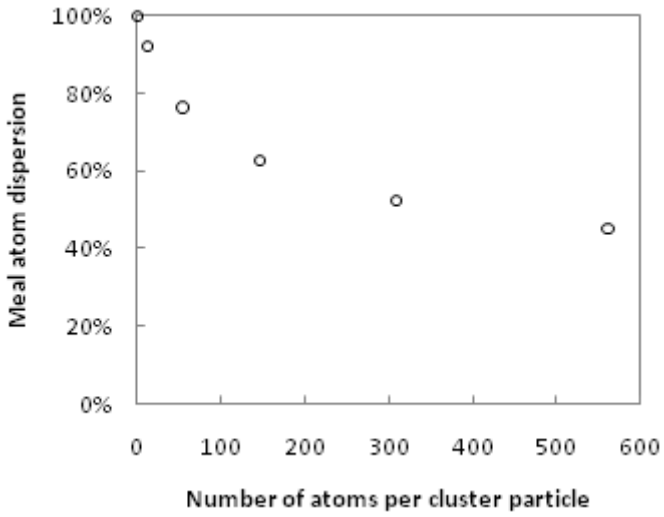

Figure A4 metal dispersion vs particle s 1

Appendice B

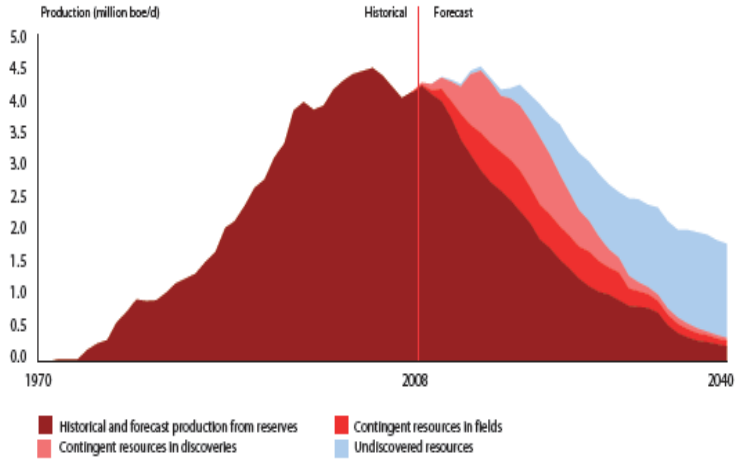

Figure 1.1.2 crude oil production forecast [26]

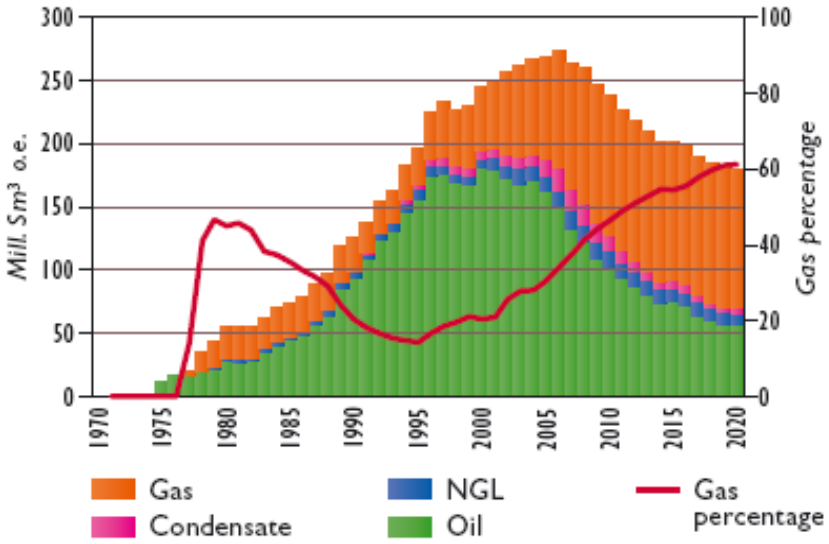

Figure 1.1.3 production forecast of gas and oil [26][27]

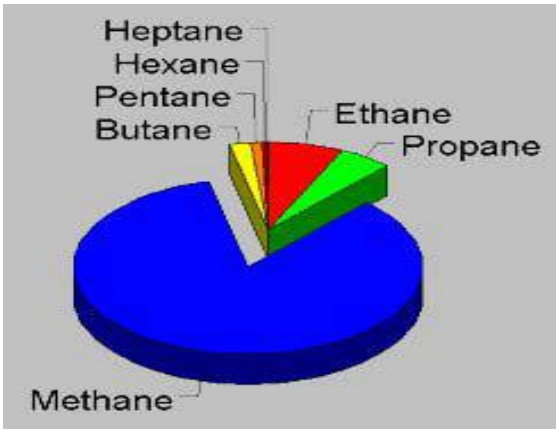

Figure1.1.4 natural gas content [1]

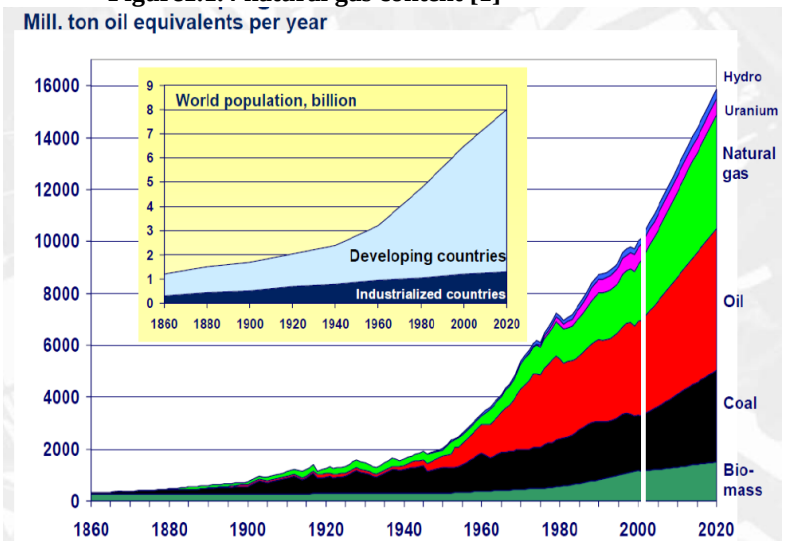

Figure 1.1.1 world energy consumption and population increase [1]

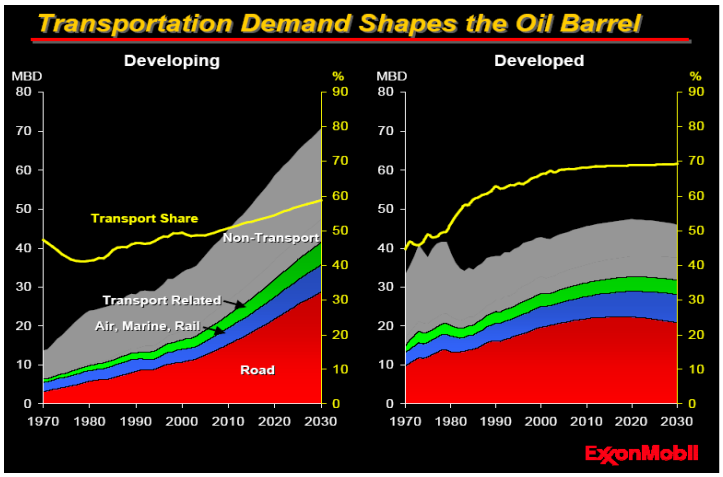

Figure1.1.2 Transportation demand [2]

Figure 3.1 Micromeritic ASAP 2010C instrument

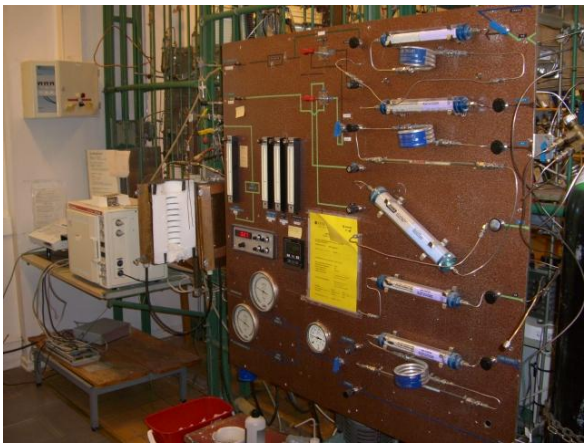

Figure 3.2 TPR instrument set up

Appendice C

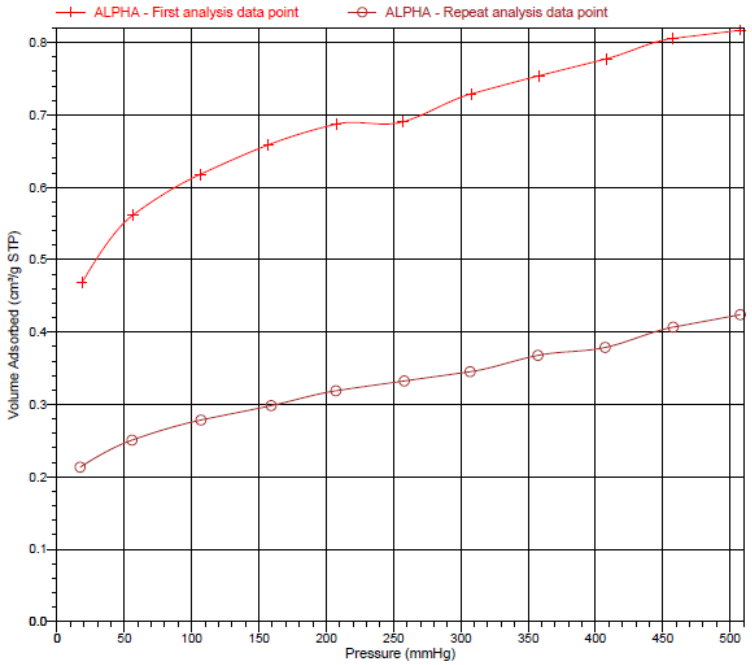

Figure 4.3a Isotherm for Co-Re/ α -Al_2O_3

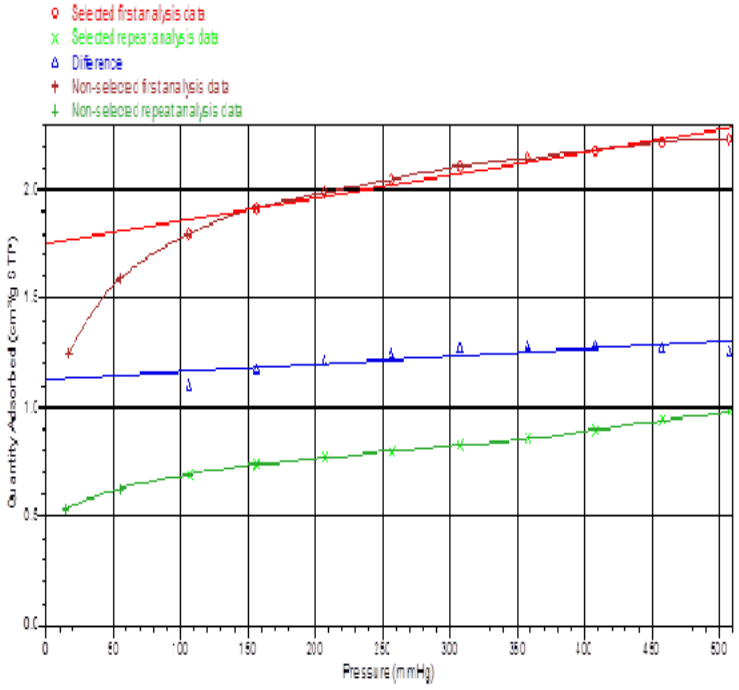

Figure 4.3b Isotherm for Co-Re/Θ- Al_2O_3

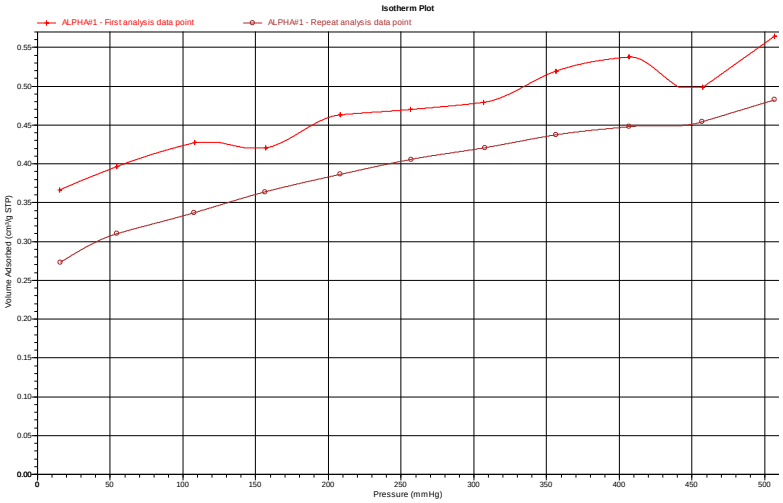

Figure 4.3c Isotherm for Co-Pt/ α -Al_2O_3

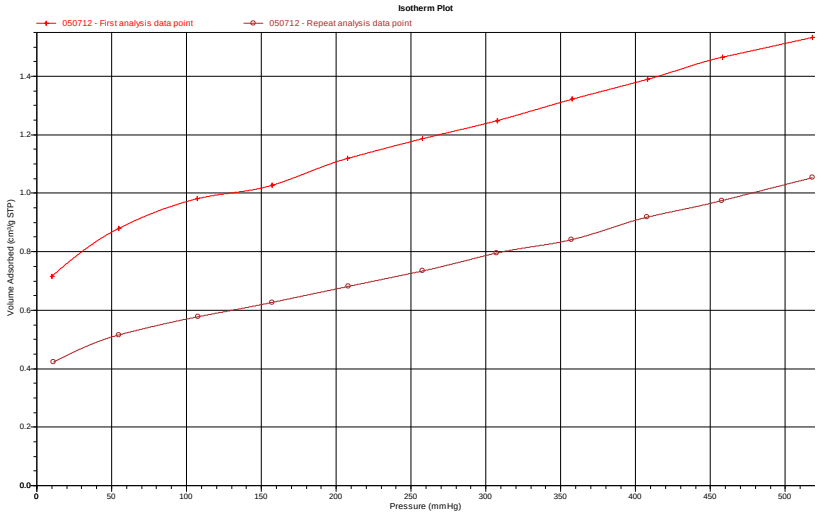

Figure 4.3d Isotherm for Co-Pt/Θ- Al_2O_3

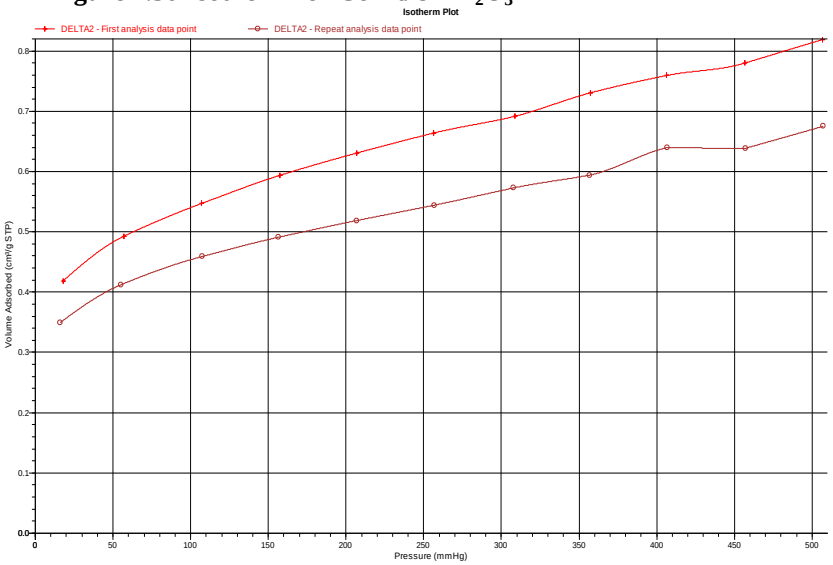

Figure 4.3e Isotherm for Co-Pt/ δ- Al_2O_3

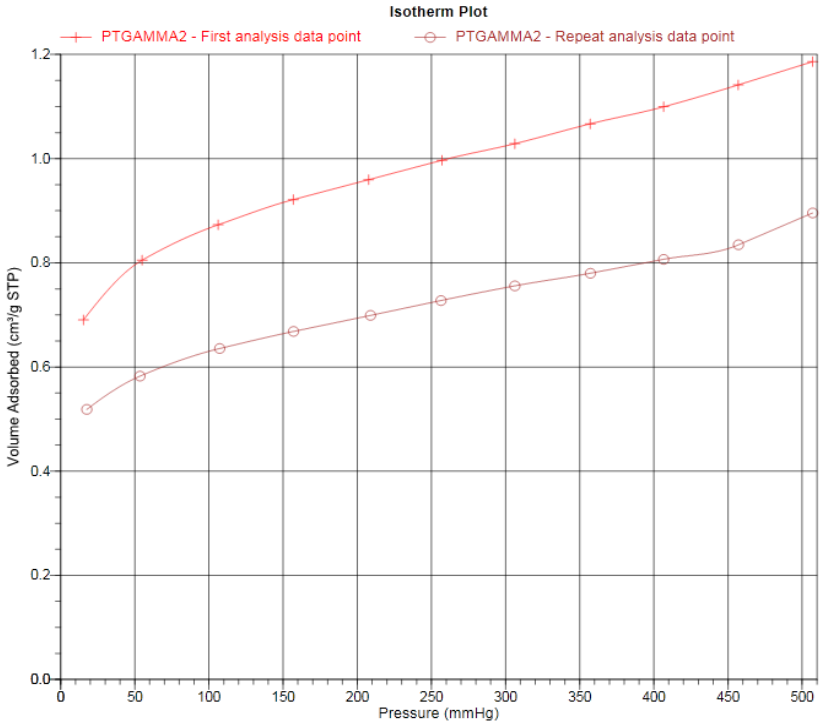

Figure 4.3f Isotherm for Co-Pt/ γ - Al2O3